表　　題　ラットＥ型肝炎ウイルスの感染細胞からの放出に関与する宿主因子の同定とその機能解析

論 文 の 区 分　博士課程

著　　者　　名　Putu Prathiwi Primadharsini

担当指導教員氏名　岡本　宏明　教授

所　　属　自治医科大学大学院医学研究科
専攻　人間生物学系
専攻分野　生体防御医学
専攻科　分子ウイルス学

２０２０年1月１０日申請の学位論文

Table of Contents

List of Abbreviations

aa	: Amino acid
Alix	: Apoptosis-linked gene 2-interacting protein X
Baf-A1	: Bafilomycin A1
BSA	: Bovine serum albumin
CHMP2A	: Charged multivesicular body protein 2A
CHMP4B	: Charged multivesicular body protein 4B
DAPI	: 4’6-diamidino-2-phenylindole
DMEM	: Dulbecco’s modified eagle medium
DMSO	: Dimethyl sulfoxide
DN	: Dominant-negative
DOC-Na	: Sodium deoxycholate
dpi	: Days post-inoculation
ESCRT	: Endosomal sorting complex required for transport
FBS	: Fetal bovine serum
HAV	: Hepatitis A virus
HCV	: Hepatitis C virus
HEV	: Hepatitis E virus
HHV-6	: Human herpes virus-6
HIV	: Human immunodeficiency virus
Hrs	: Hepatocyte growth factor-regulated tyrosine kinase substrate
HSV-1	: Herpes simplex virus-1
IDWR	: Infectious Diseases Weekly Report

IEM	: Immune electron microscopy
IFA	: Immunofluorescence assays
IgA	: Immunoglobulin A
IgG	: Immunoglobulin G
IP	: Immunoprecipitation
kb	: Kilobases
L-domain	: Late domain
mAb	: Monoclonal antibody
MEGA 7	: Molecular evolutionary genetics analysis version 7.0
MLV	: Murine leukemia virus
MTS	: 3-(4,5-dimethylthiazol-2-yl)-5-(3-carboxymethoxyphenyl)-2-(4-sulphophenyl)-2H-tetrazolium, inner salt
MVB	: Multivesicular body sorting
Nedd4	: Neural precursor cell expressed developmentally down-regulated protein 4
ORF	: Open reading frame
pAb	: Polyclonal antibody
PBS	: Phosphate-buffered saline
Rab27A	: Rab-associated binding 27A
SD	: Standard deviation
SDS-PAGE	: Sodium dodecyl sulfate-polyacrylamide gel electrophoresis
siRNA	: Small interfering RNA
TEM	: Transmission electron microscope
Tsg101	: Tumor susceptibility gene 101
UTR	: Untranslated region

Vps4	: Vacuolar protein sorting 4
WHO	: World Health Organization
wt	: Wild-type

Summary

Recent reports have shown that rat hepatitis E virus (HEV) is capable of infecting humans. Rat HEV is also successfully propagated into human PLC/PRF/5 cells, raising the possibility of a similar mechanism shared by human HEV and rat HEV. It has previously been reported that human HEV recruited tumor susceptibility gene 101 (Tsg101) via its PSAP motif in open reading frame 3 (ORF3) protein and that it required multivesicular body (MVB) sorting for virion egress. However, rat HEV ORF3 has the PxYPMP motif instead of the PSAP motif. This proline-rich sequence is indispensable for rat HEV release, although the release mechanism remains unclear. The overexpression of dominant-negative (DN) mutant of vacuolar protein sorting (Vps)4A or Vps4B decreased rat HEV release to 23.9% and 18.0%, respectively. The release of rat HEV was decreased to 8.3% in Tsg101-depleted cells and to 31.5% in apoptosis-linked gene 2-interacting protein X (Alix)-depleted cells. Although rat HEV ORF3 protein did not bind to Tsg101, I found a 90-kDa protein capable of binding to wild-type rat HEV ORF3 protein but not to ORF3 mutant with proline to leucine mutations in the PxYPMP motif. Rat HEV release was also decreased in Ras-associated binding 27A (Rab27A)- or hepatocyte growth factor-regulated tyrosine kinase substrate (Hrs)-depleted cells (to 20.1% and 18.5%, respectively). In addition, the extracellular rat HEV levels in the infected PLC/PRF/5 cells were increased after treatment with Bafilomycin A1 and decreased after treatment with GW4869. These results indicate that rat HEV utilizes MVB sorting for its release and that the exosomal pathway is required for rat HEV egress. A host protein alternative to Tsg101 that can bind to rat HEV ORF3 should be explored in further study.

1. Introduction

Hepatitis E virus (HEV) infection is distributed around the world, not only in developing countries, but also in industrialized countries [1]. The virus has a single-stranded positive-sense RNA genome ranging from 6.6 kilobases (kb) to 7.2 kb, with three open reading frames (ORFs) encoding ORF1 (non-structural protein responsible for replication), ORF2 (capsid protein) and ORF3, the multifunctional phosphoprotein that is recently found to be important for virion egress and is a functional ion channel as a viroporin (Fig. 1). HEV genome has a short 5'-untranslated region (5'-UTR) capped at its 5'-end and a short 3'-UTR terminated by poly(A) tract [2-9] (Fig. 1).

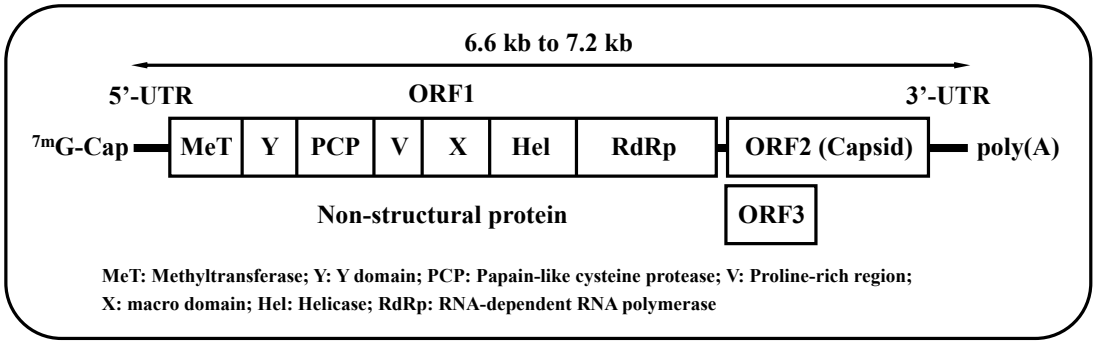

Fig. 1. HEV genome. Single-stranded positive-sense HEV RNA genome with three ORFs encoding ORF1, ORF2 and ORF3.

Around 20 million HEV cases have been reported worldwide, with 3.3 million symptomatic cases annually. By 2015, HEV infection had caused approximately 44,000 deaths as estimated by World Health Organization (WHO) [10]. In Japan, after medical insurance started covering diagnosis based on the IgA anti-HEV antibody

tests in 2011, the number of reported acute HEV infections have been increasing every year from just above 100 cases in 2012, to nearly 500 cases in 2019 [11]. HEV infection is associated with poor prognosis in pregnant women, particularly those in the third trimester, where the fatality rate could reach up to 30% [12]. HEV can cause acute and chronic infections, and chronic cases mainly occur in patients in an immunocompromised state, such as transplant recipients or human immunodeficiency virus (HIV)-infected patients [13,14]. Besides causing typical hepatitis, the infection can also result in extrahepatic manifestations, such as neurological abnormalities, hematological abnormalities and renal failure [15].

Over the past years, HEV strains have been increasingly isolated not only from humans but also from a broad range of animal species with distinct host ranges (Table 1) [1]. HEV belongs to family *Hepeviridae* [7]. The family *Hepeviridae* is divided into two genera: genus *Orthohepevirus*, which includes strains from mammals and birds; and genus *Piscihepevirus*, which only consists of species *Piscihepevirus A* with a single member, cutthroat trout HEV. Genus *Orthohepevirus* consists of four species, *Orthohepevirus A*, *Orthohepevirus B*, *Orthohepevirus C* and *Orthohepevirus D* [7] (Fig. 2). Several related *Hepeviruses* are yet to be classified, such as those from moose, fox, little egret, tree shrew, sparrow and agile frog [1].

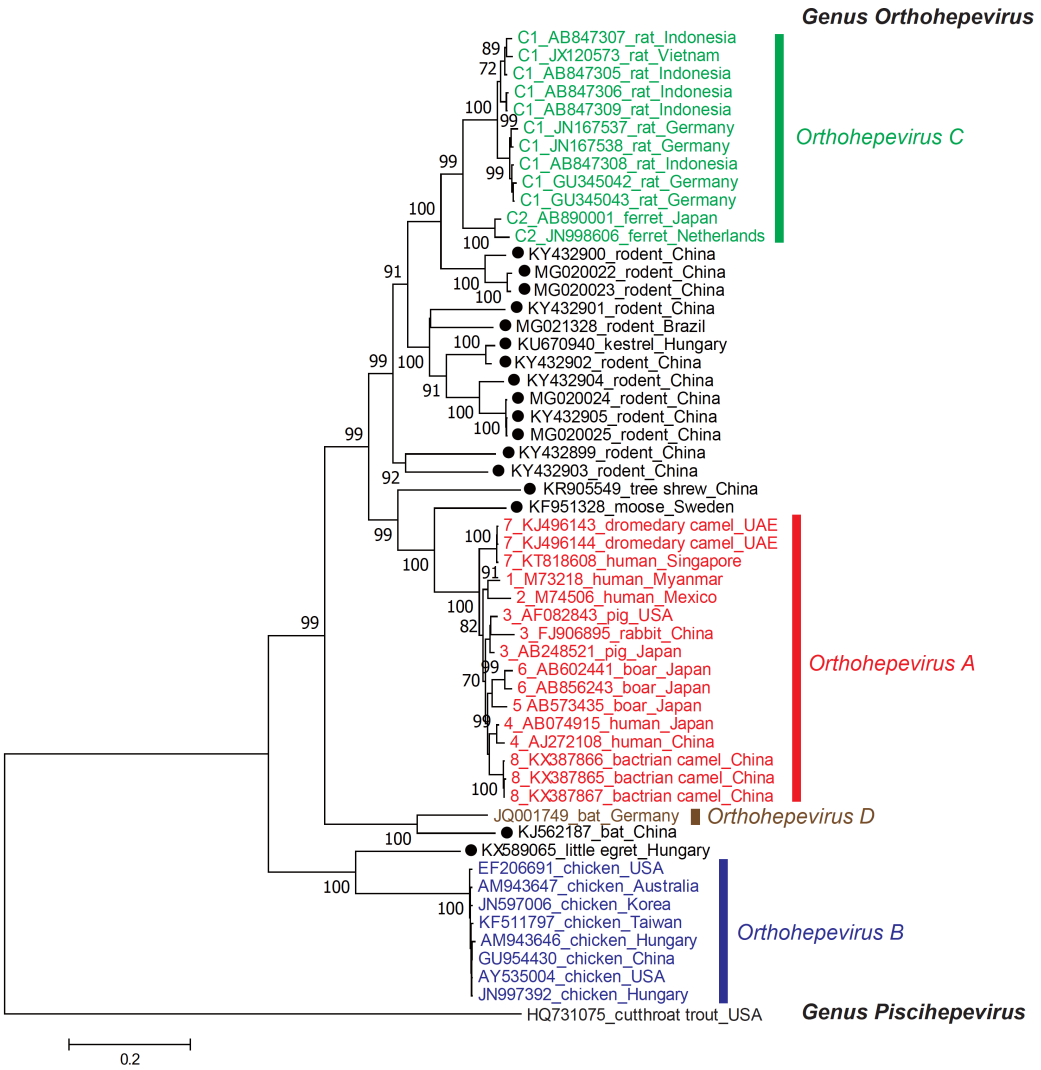

Fig. 2. Phylogenetic tree for members of the *Hepeviridae* family. The maximum-likelihood tree was created using MEGA 7 [16] based on amino acid sequences of the entire ORF2 region from members of the *Hepeviridae* family. Each reference sequence is shown with the genotype (if available) followed by the accession number, species (animal/human) and the country where it was isolated. Unassigned HEV strains are highlighted with closed circles. The bootstrap values (>70%) for the nodes are indicated as percentage data obtained from 1000 resampling analyses. The scale bar indicates the number of nucleotide substitutions per site (modified from [1]).

Previously, only four genotypes within *Orthohepevirus A* species were known to infect humans (HEV-1, HEV-2, HEV-3 and HEV-4). HEV-1 and HEV-2 are

restricted to humans. They are responsible for outbreaks in developing countries where the infection was transmitted through ingestion of contaminated water. HEV-3 and HEV-4 have been identified not only in humans but also in a variety of animal species (e.g. pig, wild boar, deer, rabbit etc.) (Table 1), and are associated with sporadic HEV infection in developed countries with variable transmission routes, mainly via a zoonotic foodborne route, with other routes being reported to be through solid-organ transplantation, transfusion of blood products, etc. [17-21]. Besides the four main genotypes, a recent report mentioned a case of patient with HEV infection caused by HEV-7 within *Orthohepevirus A* species (dromedary camel) [22]. The list is becoming even longer as two cases of human infected with rat HEV of the *Orthohepevirus C* species, were reported from an immunocompromised patient in Hong Kong and immunocompetent patient in Canada [23,24].

Table 1. Classification of *Hepeviruses* (modified from [1]).

Family	Genus	Species	Genotype	Host
Hepeviridae	*Orthohepevirus*	*Orthohepevirus A*	1	human
			2	human
			3	human, pig, wild boar, deer, mongoose, rabbit, goat, horse, bottlenose dolphin, sheep
			4	human, pig, wild boar, cattle, cow, sheep, goat, yak
			5	wild boar
			6	wild boar
			7	dromedary camel
			8	Bactrian camel
		Orthohepevirus B		chicken
		Orthohepevirus C	C1	rat, greater bandicoot rat, Asian musk shrew
			C2	ferret, mink
		Orthohepevirus D		bat
	Piscihepevirus	*Piscihepevirus A*		cutthroat trout

In enveloped viruses, the formation of an outer virion membrane is a necessary step for the completion of the virus budding. The virion membrane is often derived from host cell membranes [25]. Most enveloped viruses encode late (L)-domains in their viral genomes that can bind to the endosomal sorting complex required for transport (ESCRT) or ESCRT-associated factors of the host to facilitate viral budding. However, vacuolar protein sorting 4 (Vps4) which is a member of the AAA-ATPase family essential for cargo sorting and formation of multivesicular body (MVB), facilitates the release of ESCRT complexes from the MVB after the completion of the vesicle budding process [26-28].

At present, three L-domains [P(T/S)AP, YxxL and PPxY] have been widely studied in enveloped RNA viruses. They bind to host cellular factors [Tumor susceptibility gene 101 (Tsg101), apoptosis-linked gene 2-interacting protein X (Alix) and neural precursor cell expressed developmentally down-regulated protein 4 (Nedd4), respectively] to promote virus release [29-32]. Tsg101 is an important component of ESCRT-I, while Alix and Nedd4 are known to be ESCRT-associated adaptors [27,28,32].

Exosomes are a subtype of microvesicle with many varying downstream effects and originate within the MVB. Their size ranges from 30 to 100 nm. Exosomes have been implicated in a variety of viral pathologies [33,34]. Some viruses hijack members of ESCRT and the vesicular trafficking machinery, thus integrating their viral components into exosomes for release through the exosomal pathway [35].

HEV was originally recognized as a non-enveloped virus detected in the bile and feces of infected individuals. However, previous studies showed that, in the bloodstream and culture supernatant HEV particles are covered by a cellular membrane and ORF3 protein and termed membrane-associated HEV particles [36-

38] (Fig. 3). In infected hosts, HEV particles exist in two distinct forms where they enter the bloodstream in membrane-associated form and are excreted through the feces in membrane-unassociated form [36,37] (Fig. 4). It has also been reported that PSAP motif in human HEV ORF3 protein is required for the formation of membrane-associated particles by interacting with host factor Tsg101, and that human HEV required MVB sorting and the exosomal pathway for virion egress [39,40].

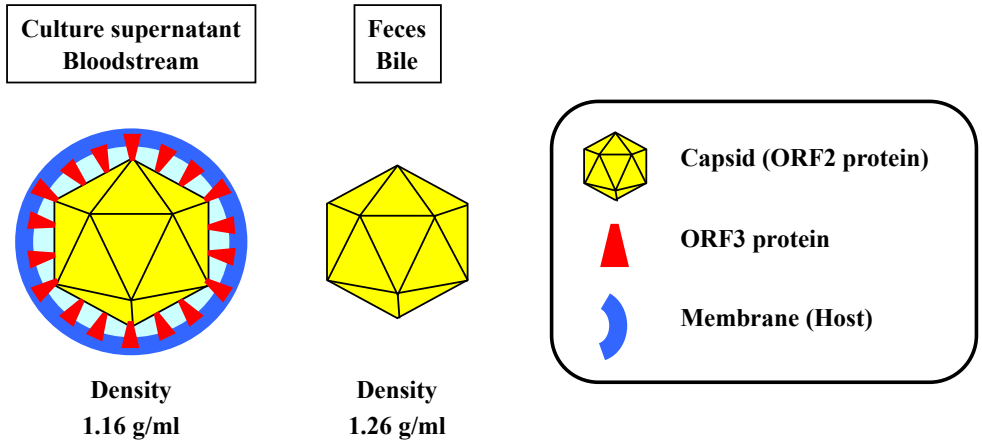

Fig. 3. Schematic diagrams of HEV particles. HEV particles in feces are non-enveloped, while those in culture supernatant and circulating blood are covered by a cellular membrane and ORF3 protein.

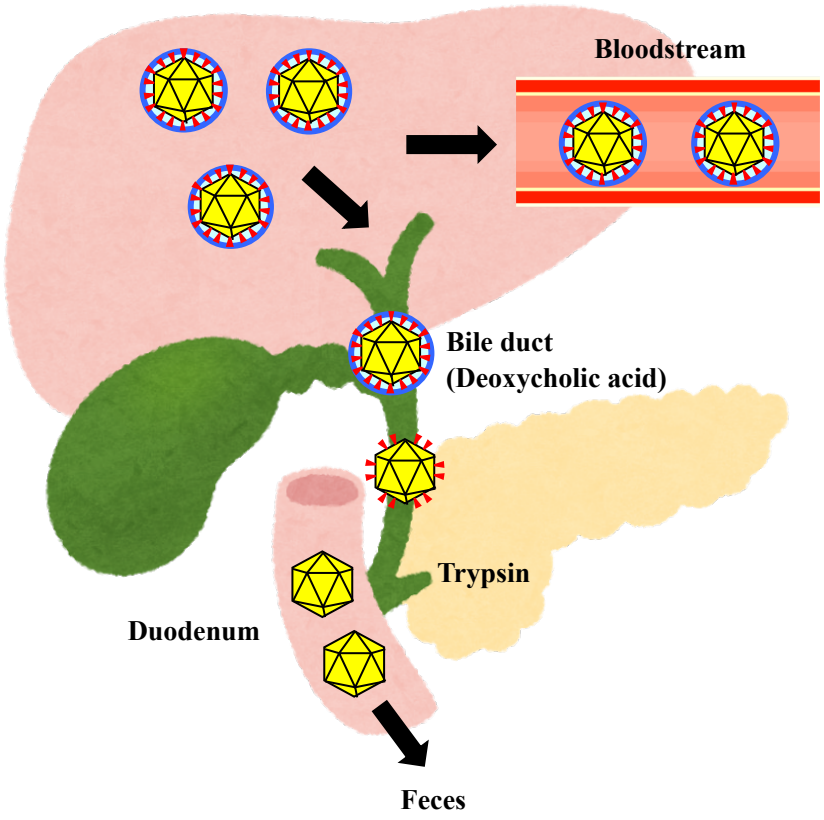

Fig. 4. The presence of two distinct forms of HEV particles in infected hosts. In the bloodstream, HEV particles are covered by the lipid membrane and ORF3 protein. The lipid membrane is removed by deoxycholic acid in the bile duct followed by the removal of ORF3 protein in the duodenum by the trypsin secreted from pancreas. The virus particles are finally excreted as non-enveloped virus in the feces.

Rat HEV has been identified around the world [41]. It belongs to *Orthohepevirus C* species with a genomic length of 6.9 kb [7]. Rat HEV is capable of infecting humans [23,24]. Rat HEV is also successfully propagated in PLC/PRF/5 cells derived from human hepatocellular carcinoma [42]. Although it was shown that ORF3 protein, especially its proline-rich sequence (PxYPMP), is important for rat HEV egress (Fig. 5) [43], the mechanism underlying rat HEV egress from infected cells and the host factors associated with rat HEV release remain unclear.

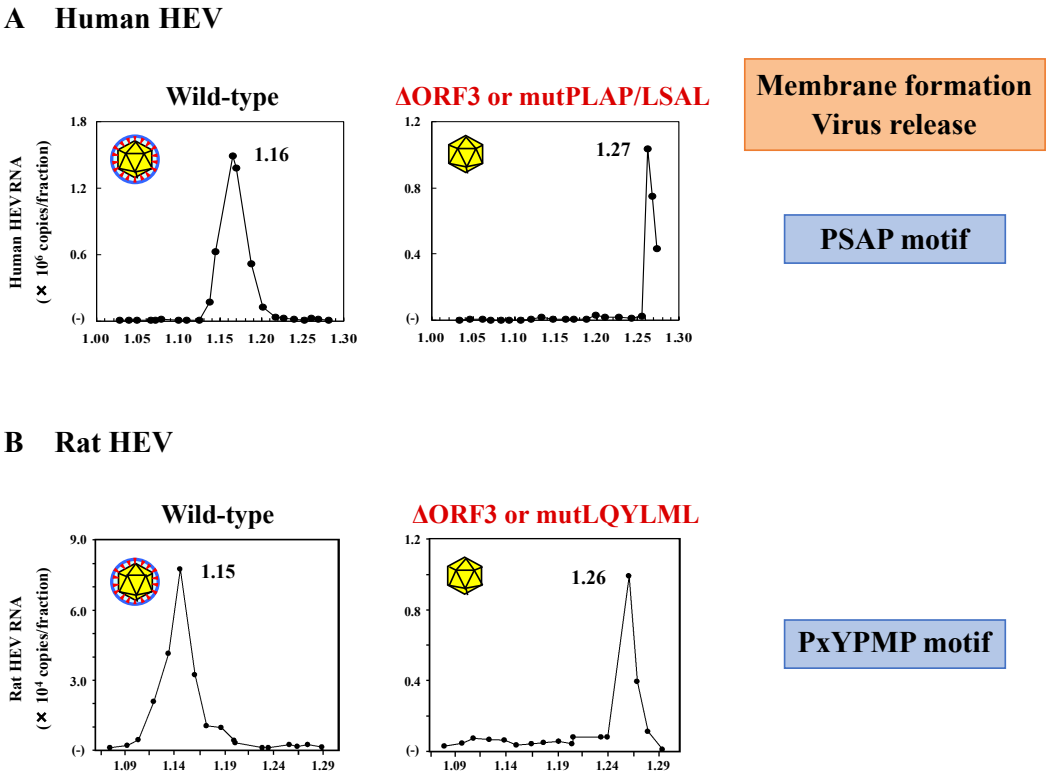

Fig. 5. Roles of ORF3 protein in human and rat HEV. ORF3 protein plays important roles in both human and rat HEV for membrane formation and the virus release. Particularly, these functions belong to PSAP motif in human HEV ORF3 (A) [5] or PxYPMP motif in rat HEV ORF3 (B) [43].

In the present study, I investigated whether or not rat HEV has a similar release mechanism to human HEV by studying the utilization of MVB sorting and the exosomal pathway for rat HEV release from infected cells. I also explored the host cellular factors associated with this event.

2. Materials and Methods

2.1. Cell culture

PLC/PRF/5 cells obtained from the American Type Culture Collection (ATCC no. CRL-8024, Manassas, VA) were grown in Dulbecco's Modified Eagle Medium (DMEM) (Thermo Fisher Scientific, Waltham, MA) containing 10% (v/v) heat-inactivated fetal bovine serum (FBS) (Thermo Fisher Scientific), 100 U/ml penicillin G, 100 μg/ml streptomycin and 2.5 μg/ml amphotericin B (growth medium) at 37°C in a humidified 5% CO_2 atmosphere, as described previously [44]. For experiments using rat HEV, the growth medium was supplemented with 1% (v/v) dimethyl sulfoxide (DMSO) (Nacalai Tesque, Kyoto, Japan) (growth medium + 1% DMSO).

2.2. Viruses

The cell-culture derived ratELOMB-131L strain (1.2×10^8 copies/ml) [42] or culture supernatants containing a cell-culture adapted genotype 3 JE03-1760F strain (passage 26; 4.3×10^7 copies/ml) [45] were used in this study.

2.3. Transmission electron microscopy (TEM)

Membrane-associated rat HEV particles were purified by ultracentrifugation as previously described [38]. In brief, culture supernatants of rat HEV-infected PLC/PRF/5 cells were filtered through a 0.22 μM filter (Merck-Millipore, Burlington, MA) then ultracentrifuged at 100,000*g* for 70 min at 4°C (Beckman Coulter, Miami, FL). Membrane-unassociated rat HEV particles were generated by treating the exosome fraction of the rat HEV-infected PLC/PRF/5 cells with 0.2% sodium

deoxycholate (DOC-Na) and 0.2% Trypsin in phosphate-buffered saline (pH 7.5) without Mg^{2+} and Ca^{2+} [PBS(-)] at 37°C for 5 h and pelleted through a 30% cushion at 270,000*g* for 4 h at 4°C. The pellet was washed with PBS(-). After washed, the pellet was resuspended in PBS(-) and stored at 4°C until use.

The membrane-associated and membrane-unassociated rat HEV particles were allowed to adsorb for 1 min onto Formvar-coated grids. Excess solution was absorbed with filter paper. The rat HEV particles were negatively stained with 1% uranyl acetate for 1 min and observed under TEM HT7600 (Hitachi, Tokyo, Japan) at an acceleration voltage of 80 kV. One hundred and fifty particles were used to calculate the diameter of each particle form and presented as the mean ± standard deviation (SD) (nm).

2.4. Immune electron microscopy (IEM)

Immunogold labelling was performed in accordance with the previously described method [38]. Briefly, Formvar-coated nickel grids were floated on drops of the viral suspensions (obtained from the methods above) for 20 min. The grids were then treated with PBS(-) containing 1% (v/v) bovine serum albumin (BSA) (Thermo Fisher Scientific) for 20 min, followed by application of the primary antibody [anti-rat HEV ORF2 monoclonal antibody (mAb) (TA7005, mouse IgG) [46] or anti-rat HEV ORF3 mAb (TA7126, mouse IgG) [47] at 1/50 dilution in PBS(-) containing 0.2% BSA] and incubated for 1 h at room temperature. After washing five times with PBS(-) containing 0.2% (v/v) BSA, colloidal gold-conjugated secondary antibody was incubated with the grids for 2 h [1/20 dilution of goat anti-mouse IgG conjugated with 12 nm-colloidal gold (Jackson ImmunoResearch Laboratories, West Grove, PA)] in PBS(-) containing 0.2% BSA. The grids were washed five times with 0.2% BSA

in PBS(-) and rinsed three times with PBS(-). In the final step, the grids were negatively stained with 1% uranyl acetate for 1 min and observed under TEM, as described above.

2.5. Plasmids

Plasmids that express FLAG-tagged Vps4 (pVps4A and pVps4B) and dominant-negative (DN) mutants of Vps4A and Vps4B, termed pVps4AEQ (E228Q) and pVps4BEQ (E235Q), respectively, have been described previously [48]. Plasmids that express DN mutant of Nedd4 (pNedd4.1-WW) has also been described previously [49].

2.6. Virus inoculation

Monolayers of PLC/PRF/5 cells in 24-well plates (Thermo Fisher Scientific) were inoculated with 1×10^6 copies/well of ratELOMB-131L or 2×10^5 copies/well of JE03-1760F diluted with PBS(-) containing 0.2% BSA. After 1 h of inoculation at room temperature, the cells were washed with PBS(-), 0.5 ml growth medium or growth medium + 1% DMSO was added to each well, and the cells were incubated at 37°C. Every other day, half of the culture medium (0.25 ml) of the infected cells was replaced with growth medium or growth medium + 1% DMSO. The collected culture medium was centrifugated at 1,300*g* at room temperature for 2 min, and then the supernatant was stored at -80°C until use.

2.7. Plasmid transfection

To analyze the effects of the overexpression of Vps4 DN mutants on the release of rat HEV, PLC/PRF/5 cells (1×10^5 cells/well) in 24-well plates were transfected with 0.5 μg of the expression plasmids for wild-type Vps4 (Vps4A or Vps4B) or their DN mutants (Vps4AEQ or Vps4BEQ) using TransIT-LT1 reagent (Mirus Bio, Madison, WI) according to the manufacturer's instructions. The overexpression of DN mutant of Nedd4 (Nedd4-WW) was performed via similar methods, as described above. Empty vector was used as a control in the respective experiments.

2.8. RNA interference

The small interfering RNAs (siRNAs) (Horizon Discovery, Cambridge, UK) used in this study were human Tsg101 (siGENOME SMARTpool M-003549), human Alix (siGENOME SMARTpool M-004233), human Nedd4 (siGENOME SMARTpool M-007178), human Ras-associated binding 27A (Rab27A) (siGENOME SMARTpool M-004667), human hepatocyte growth factor-regulated tyrosine kinase substrate (Hrs) (siGENOME SMARTpool M-016835) and control siRNA (siGENOME Non-Targeting siRNA Pool #1 D-001206). PLC/PRF/5 cells with a density of 1×10^5 cells/well were seeded into 24-well plates in antibiotic-free growth medium and incubated at 37°C for 24 h. The cells were transfected with 5 nM siRNA (final concentration) in Opti-MEM (Thermo Fisher Scientific) using DharmaFECT 1 reagent (Horizon Discovery) according to the manufacturer's instructions.

2.9. Western blotting

To check the expression of cells transfected with expression plasmid or siRNA, cells were lysed in lysis buffer [50 mM Tris/HCl (pH 8.0), 1% (v/v) NP-40, 150 mM NaCl and protease inhibitor cocktail (Nacalai Tesque)]. The proteins in the cell lysates were separated by sodium dodecyl sulfate-polyacrylamide gel electrophoresis (SDS-PAGE) and blotted onto PVDF membranes (0.45 μM) (Merck-Millipore, Burlington, MA), immunodetected with specific antibodies and visualized by a chemiluminescence assay using SuperSignal West Femto Chemiluminescent Substrate (Thermo Fisher Scientific) with an ImageQuant LAS 500 (GE Healthcare, Chicago, IL), as described previously [4]. The primary antibodies used were as follows: anti-Tsg101 mouse mAb (Santa Cruz Biotechnology, Santa Cruz, CA), anti-Alix rabbit polyclonal antibody (pAb) (Sigma-Aldrich Merck, Darmstadt, Germany), anti-Nedd4 rabbit pAb (Proteintech, Rosemont, IL), anti-Rab27A mouse mAb (Sigma-Aldrich Merck), anti-Hrs mouse mAb (Sigma-Aldrich Merck), anti-rat HEV ORF3 rabbit pAb (JB761) [43], anti-human HEV ORF3 mouse mAb (TA0536) [36], anti-FLAG mouse mAb (Sigma-Aldrich Merck) or rabbit pAb (Proteintech), or anti-Myc mouse mAb (Santa Cruz Biotechnology).

2.10. Quantitation of rat HEV RNA or human HEV RNA

Total RNA was extracted from culture supernatant by TRIzol-LS reagent (Thermo Fisher Scientific) or cells by TRIzol reagent (Thermo Fisher Scientific). The quantitation of rat HEV RNA or human HEV RNA was performed by real-time reverse transcription polymerase chain reaction (RT-PCR), using a LightCycler apparatus (Roche, Mannheim, Germany), a QuantiTect Probe RT-PCR kit (Qiagen,

Hilden, Germany) and primer sets and probe targeting the 5'-terminal rat HEV ORF1 region [50] or human HEV ORF2 and ORF3 overlapping region [51], according to the previously described methods.

2.11. Immunofluorescence assays (IFA)

Rat HEV-infected PLC/PRF/5 cells seeded into 4-wells chamber slides (Thermo Fisher Scientific) were fixed in 4% (v/v) paraformaldehyde (FujiFilm Wako, Osaka, Japan) at room temperature for 15 min then permeabilized with PBS(-) containing 0.2% (v/v) Triton X-100 (FujiFilm Wako) at room temperature for 10 min. Non-specific binding was blocked with 1% BSA in PBS(-) at room temperature for 30 min. The fixed cells were incubated with appropriate primary antibody diluted in PBS(-) containing 1% BSA at 37°C for 1 h. The primary antibodies used were anti-rat HEV ORF2 mouse mAb (TA7005), anti-rat HEV ORF3 mouse mAb (TA7126) or rabbit pAb (JB761), anti-Rab27A mouse mAb, anti-Hrs mouse mAb, anti-Tsg101 mouse mAb, anti-Alix rabbit pAb, or anti-CD63 rabbit pAb (Santa Cruz Biotechnology) or goat pAb (Santa Cruz Biotechnology). After washed with PBS(-), the cells were stained with appropriate secondary antibody diluted in PBS(-) containing 1% BSA at 37°C for 1 h. The secondary antibodies used (Thermo Fisher Scientific) were Alexa Fluor 488-conjugated anti-mouse IgG or anti-rabbit IgG, Alexa Fluor 594-conjugated anti-mouse or anti-rabbit IgG, Alexa Fluor 555-conjugated anti-goat IgG or Alexa-Fluor 350-conjugated anti-goat IgG according to the primary antibodies used. The nuclei were counterstained with 4'6-diamidino-2-phenylindole (DAPI: Thermo Fisher Scientific). The slide glasses were mounted with Fluoromount/Plus medium (Diagnostic BioSystems, Pleasanton, CA) and then viewed under an FV1000 confocal laser microscope (Olympus, Tokyo, Japan).

2.12. Treatment of rat HEV-infected PLC/PRF/5 cells with accelerator or inhibitor of exosome release

Monolayers of rat HEV-infected PLC/PRF/5 cells grown on 24-well plates were washed with PBS(-) and incubated with the indicated concentrations of Bafilomycin A1 (Baf-A1; BioViotica, Liestal, Switzerland) or GW4869 (Cayman Chemical, Ann Arbor, MI) in growth medium containing 1% DMSO (final concentration). After 24 h of incubation at 35.5°C, the culture supernatant was collected and centrifuged at 1,300*g* at room temperature for 2 min; and the supernatant was then stored at -80°C until use. The cells were washed and collected in the presence of TRIzol reagent. The samples were stored at -80°C until use.

2.13. MTS assays

Monolayers of PLC/PRF/5 cells in 96-well plates (Thermo Fisher Scientific) were incubated with growth medium containing the indicated concentrations of Baf-A1, GW4869 or DMSO at 35.5°C. After 24 h of incubation, the number of viable cells was measured by the 3-(4,5-dimethylthiazol-2-yl)-5-(3-carboxymethoxyphenyl)-2-(4-sulphophenyl)-2H-tetrazolium, inner salt (MTS) assay using a CellTiter 96® AQueous One Solution Cell Proliferation Assay (Promega, Madison, WI) according to the manufacturer's instructions.

2.14. Immunoprecipitation (IP) assays

PLC/PRF/5 cells were transfected with pCI-ratHEV ORF3-G2, which is an expression plasmid for the full-length rat HEV ORF3 protein [47] or pCI-HEVORF3/wt [36], which is an expression plasmid for the full-length human HEV

ORF3 protein, using the TransIT-LT1 reagent according to the manufacturer's instructions. At 48 h after transfection, co-IP assays were performed using an Immunoprecipitation Kit (Protein G) (Roche, Mannheim, Germany) according to the manufacturer's instructions. After clarification by centrifugation, cell lysates were subjected to IP with anti-Tsg101 goat pAb (Santa Cruz Biotechnology), anti-Alix rabbit pAb, anti-Nedd4 rabbit pAb, anti-rat HEV ORF3 rabbit pAb (JB761) or anti-human HEV ORF3 mouse mAb (TA0536). The co-immunoprecipitated proteins were separated by 15% SDS-PAGE, followed by Western blotting with an anti-rat HEV ORF3 rabbit pAb (JB761) or anti-human HEV ORF3 mouse mAb (TA0536), as described above.

2.15. Construction of tagged rat HEV ORF3 and its mutant

First, the expression plasmid for FLAG- and Myc-tagged rat HEV ORF3 (pFLAG-Myc-CMV22-rat HEV ORF3_wt) was constructed as follows: the coding sequence of rat HEV ORF3 gene was amplified by PCR using infectious cDNA clone of ratELOMB-131L as a template [42], KOD Plus DNA polymerase (Toyobo, Osaka, Japan) and appropriate oligonucleotide primers. The sequences of the primers used were as follows: EcoRI-A-ratORF3-4956P, 5'-TGAATTCAATGTGCGCGAAATGTCTGTCG-3'; *Eco*RI site (underlined) and plus-strand sequence (nt 4956-4976) of ratELOMB-131L, and XbaI-ratORF3-5261M, 5'-ATCTAGATTGGCGACTGCCCGGCATCG-3'; *Xba*I site (underlined) and minus-strand sequence (nt 5242-5261) of ratELOMB-131L. The PCR product was digested with *Eco*RI (New England BioLabs, Ipswich, MA) and *Xba*I (New England BioLabs). The *Eco*RI-*Xba*I fragment was ligated into pFLAG-Myc-CMV-22 (Sigma-Aldrich Merck), from which the *Eco*RI-*Xba*I fragment had been removed, yielding

pFLAG-Myc-CMV22-rat HEV ORF3. The nucleotide sequence between the *Eco*RI and *Xba*I sites of the yielded clone was confirmed.

Next, the coding sequence of rat HEV ORF3 including the FLAG or Myc sequence was amplified by PCR using pFLAG-Myc-CMV22-rat HEV ORF3 as a template, KOD Plus DNA polymerase and appropriate oligonucleotide primers. The sequences of the primers used for FLAG-tagged rat HEV ORF3 were as follows. NheI-Kozak-FLAG, 5'-TGCTAGCCACCATGGACTACAAAGACGATG-3'; *Nhe*I site (underlined) and FLAG peptide sequence, and MluI-Stop-ratORF3-5261M, 5'-TACGCGTTCATTGGCGACTGCCCGG-3'; *Mlu*I site (underlined) and minus-strand sequence (nt 5247-5261) of rat HEV ORF3. Meanwhile, the sequences of the primers used for Myc-tagged rat HEV ORF3 were as follows: NheI-Kozak-ratORF3-4956P, 5'-TGCTAGCCACCATGTGCGCGAAATGTCTGT-3'; *Nhe*I site (underlined) and plus-strand sequence (nt 4956-4974) of ratELOMB-131L, and MluI-Stop-Myc, 5'-AACGCGTTCACAGATCCTCTTCTGAGATGA-3'; *Mlu*I site (underlined) and c-Myc sequence. The PCR products were digested with *Nhe*I (New England BioLabs) and *Mlu*I-HF (New England Biolabs). The *Nhe*I-*Mlu*I fragments were each ligated into pCI Vector (Promega), from which the *Nhe*I-*Mlu*I fragments had been removed, yielding pCI-FLAG-rat HEV ORF3 wild-type or pCI-rat HEV ORF3 wild-type-Myc. The nucleotide sequence between *Nhe*I and *Mlu*I sites of the yielded clone was confirmed.

To construct variants of ratELOMB-131L with three mutations from proline to leucine (aa 93, 96 and 98) in the proline-rich region (PxYPMP to LxYLML) of rat HEV ORF3 protein, inverse PCR was performed according to the previously described methods [52] using the yielded pCI-FLAG-rat HEV ORF3 wild-type or pCI-rat HEV ORF3 wild-type-Myc, KOD Plus version 2 DNA polymerase (Toyobo)

and appropriate oligonucleotide primers. The primer pairs used were as follows: ratElo-131L-pro-F123 and ratElo-131L-proR123 [43]. The PCR products were ligated, and the resulting clones were subjected to nucleotide sequencing to confirm the presence of expected mutations and absence of other unexpected mutations between *Nhe*I and *Mlu*I sites including the FLAG or c-Myc sequences and rat HEV ORF3 sequences. The yielded subclones were then digested with *Nhe*I and *Mlu*I-HF. The *Nhe*I-*Mlu*I fragments were each ligated into pCI Vector from which the *Nhe*I-*Mlu*I fragments had been removed, yielding pCI-FLAG-rat HEV ORF3 mutant or pCI-rat HEV ORF3 mutant-Myc. The protein expression was confirmed by plasmid transfection followed by Western blotting, as described above.

2.16. Exploration of host cellular proteins that bind to rat HEV ORF3 protein by co-IP

PLC/PRF/5 cells were transfected with pCI-FLAG-rat HEV ORF3 wild-type, pCI-FLAG-rat HEV ORF3 mutant, pCI-rat HEV ORF3 wild-type-Myc, pCI-rat HEV ORF3 mutant-Myc or pCI Vector using TransIT-LT1 reagent. At 48 h after transfection, lysates were co-immunoprecipitated with anti-FLAG mouse mAb or anti-Myc mouse mAb according to the methods described above. Co-immunoprecipitated proteins were separated by SDS-PAGE, followed by silver staining using EzStain Silver kit (ATTO, Tokyo, Japan) according to the manufacturer's instructions.

2.17. Statistical analysis

The results were presented as the mean ± SD. Statistical significance was assessed by Student's *t*-test. *P* values of less than 0.05 were considered significant.

3. Results

3.1. Morphological analyses of rat HEV particles

Previous studies reported that rat HEV particles in the serum and culture supernatant banded at a density of 1.16 g/ml in a sucrose density gradient, while those in the fecal suspension peaked at a density of 1.26 g/ml [42,47] (Fig. 3). In addition, rat HEV particles in the liver homogenates exhibited two peaks at a density of 1.13-1.15 g/ml and 1.25-1.27 g/ml [42], suggesting that the membrane-associated particles are formed intracellularly, similar to those of human HEV. In human HEV, membrane-associated HEV particles in culture supernatant are efficiently recovered in the exosome fraction [38]. In the current study, the exosome fraction was purified from culture supernatants of rat HEV-infected cells and subjected to TEM after negative staining. Virus-like particles with an average diameter of 40.6 ± 0.9 nm (n = 150) were observed in the exosome fraction (Fig. 6A). To characterize these virus-like particles, the exosome fraction was treated with 0.2% DOC-Na and 0.2% trypsin. A large number of virus-like particles with an average diameter of 26.1 ± 1.2 nm (n = 150) were observed in the purified preparations after treatment (Fig. 6B). To further demonstrate that these particles were membrane-unassociated rat HEV, additional observation was performed using immunogold labelling. The virus-like particles were clearly coated with anti-rat HEV ORF2 mAb (Fig. 6C, upper panel) but did not bind to anti-rat HEV ORF3 mAb (Fig. 6C, lower panel). These results indicated that the treated particles were membrane-unassociated rat HEV particles, further confirming that the rat HEV particles in exosome fraction are membrane-associated.

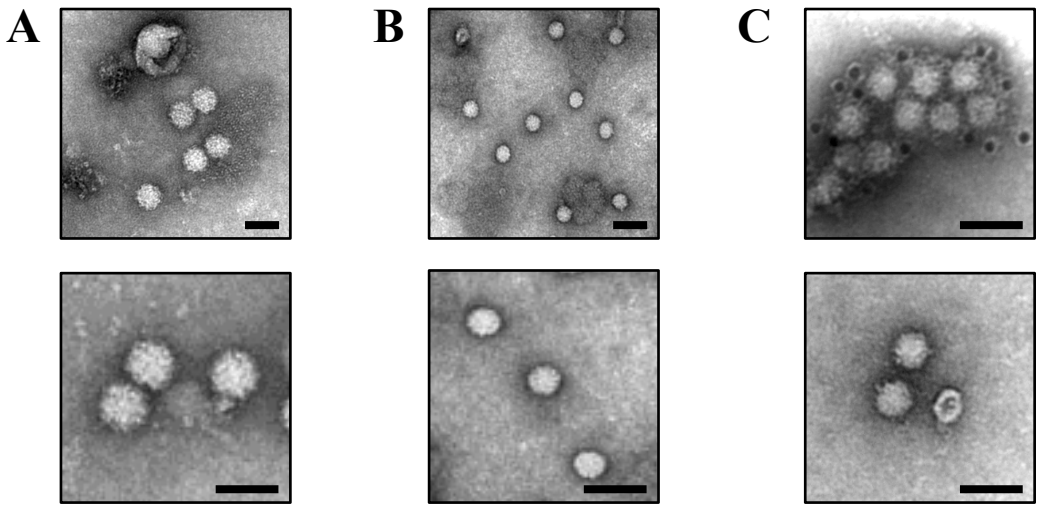

Fig. 6. Observation of two distinct forms of rat HEV particles by TEM. (A) TEM images of negatively stained membrane-associated rat HEV particles in the exosome fraction of culture supernatant and (B) membrane-unassociated rat HEV particles in the exosome fraction after treatment with 0.2% DOC-Na and 0.2% Trypsin. (C) Immunogold labeling of the membrane-unassociated rat HEV particles with anti-rat HEV ORF2 mAb (upper panel) and anti-rat HEV ORF3 mAb (lower panel). The membrane-unassociated rat HEV particles were incubated with anti-rat HEV ORF2 mAb or anti-rat HEV ORF3 mAb and a 12-nm colloidal gold-conjugated goat anti-mouse IgG. Bars, 50 nm. Results representative of one of two experiments are shown.

3.2. Effects of the overexpression of DN mutants of Vps4A or Vps4B

To analyze the utilization of MVB sorting by rat HEV for its egress, overexpression of DN mutants of Vps4A and Vps4B which are known as the final effector of this pathway were performed [48]. PLC/PRF/5 cells were transfected with 0.5 μg of empty vector or expression plasmids for the DN mutants of Vps4A or Vps4B (termed Vps4AEQ or Vps4BEQ, respectively) 2 days before inoculation. Transfection was then performed at 2, 6 and 10 days after inoculation (Fig. 7A). Two days after the first transfection, the pretreated cells were inoculated with 1×10^6

copies/ml of cell culture-derived rat HEV. The expression of Vps4AEQ and Vps4BEQ (Fig. 7B) was maintained at least until 12 days post-inoculation (dpi). The rat HEV RNA levels in the culture supernatant of the cells transfected with the empty vector increased gradually from 2 dpi and reached 8.8×10^4 copies/ml at 12 dpi. In contrast, the rat HEV RNA levels in the culture supernatant of cells transfected with Vps4AEQ or Vps4BEQ at 12 dpi were significantly decreased compared to that of empty vector, at 2.2×10^4 copies/ml (23.9%) and 1.7×10^4 copies/ml (18.0%), respectively ($p < 0.001$; Fig. 7D), indicating that the enzymatic activities of Vps4A and Vps4B are necessary for rat HEV egress.

To further investigate the functions of Vps4A and Vps4B, PLC/PRF/5 cells were transfected with 0.5 μg of empty vector or expression plasmids for the wild-type forms of Vps4A or Vps4B 2 days before inoculation. Transfection was then performed at 2, 6 and 10 dpi (Fig. 7A). Two days after the first transfection, the pretreated cells were inoculated with 1×10^6 copies/ml of cell culture-derived rat HEV. The expression of Vps4A and Vps4B (Fig. 7C) was maintained at least until 12 dpi. The rat HEV RNA levels in culture supernatant of cells transfected with the wild-type forms of Vps4A (1.3×10^5 copies/ml) or Vps4B (1.3×10^5 copies/ml) did not differ from that of empty vector (1.2×10^5 copies/ml) at 12 dpi (104.1%, $p = 0.45$; and 104.9%, $p = 0.47$, respectively) (Fig. 7E), indicating that the overexpression of wild-type forms of Vps4A and Vps4B did not affect the rat HEV release and that the endogenous Vps4 content was sufficient to produce viral particles.

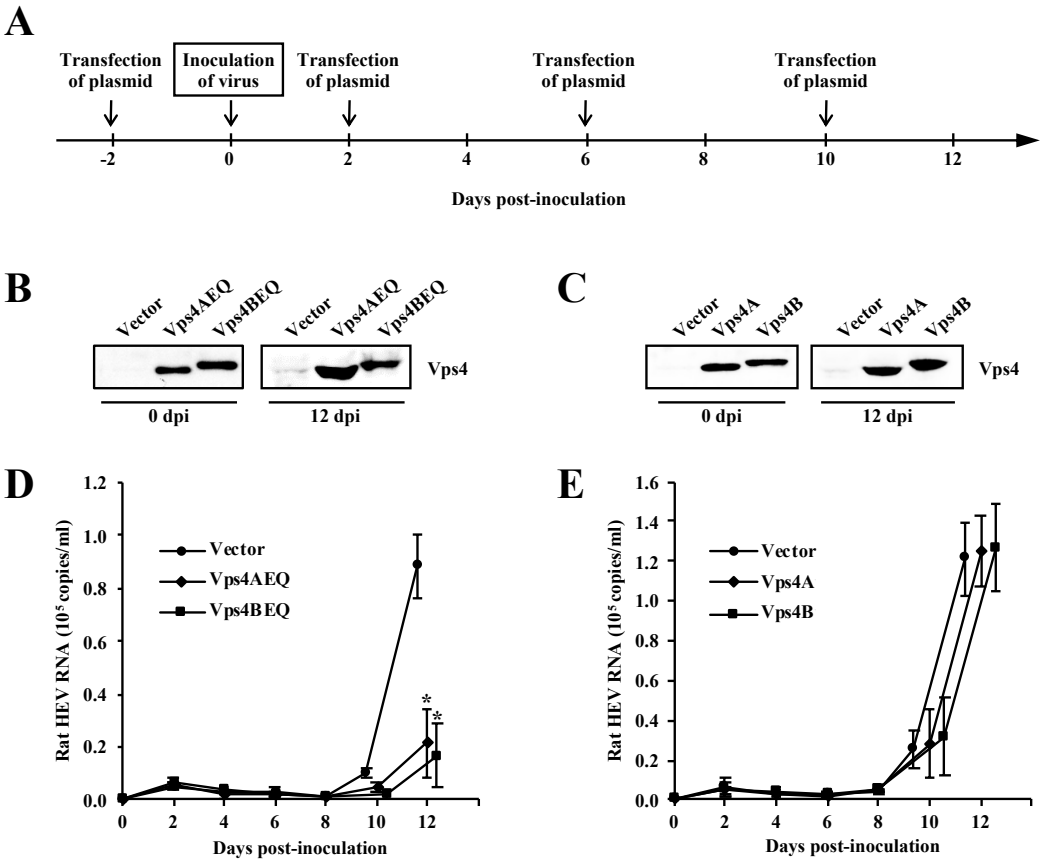

Fig. 7. Effects of Vps4 on rat HEV release. (A) The experiment schedule. PLC/PRF/5 cells were transfected with the expression plasmid 2 days before and 2, 6 and 10 days after inoculation on day 0. (B, C) The expression of DN mutants or wild-type forms of Vps4. PLC/PRF/5 cells were transfected with the Vps4AEQ, Vps4BEQ or empty vector, and Vps4A, Vps4B or empty vector. On the indicated days after inoculation, the cells were lysed and the FLAG-tagged DN mutants (B) or wild-type forms (C) of Vps4, or empty vector were subjected to Western blotting with anti-FLAG pAb. (D, E) The levels of extracellular rat HEV RNA in cells transfected with the DN mutants (D) or wild-type forms of Vps4 (E), compared to those of empty vector. The rat HEV RNA titer was quantitated by real-time RT-PCR. The data represent the mean ± SD of three independent experiments. *$p < 0.001$.

3.3. Functional involvement of host cellular factors Tsg101, Alix and Nedd4 in rat HEV release

It was previously shown that Tsg101 is important for release of human HEV [39]. To analyze whether or not the host cellular factors Tsg101, Alix and Nedd4 are functionally involved in rat HEV release, siRNAs targeting each of them were used and their effects on the virus release were examined. For comparison, similar experiment was performed using human HEV. PLC/PRF/5 cells were treated with 5 nM of siRNA specific for Tsg101 (siTsg101), Alix (siAlix) or Nedd4 (siNedd4), or negative control siRNA (siNc) 3 days before and 4 days after virus inoculation (Fig. 8A). Three days after the first transfection, pretreated cells were inoculated with either cell culture-derived rat HEV (1×10^6 copies/ml) or human HEV (2×10^5 copies/ml). The depletion of endogenous Tsg101, Alix, or Nedd4 was maintained during the observation period (12 days for rat HEV-infected cells and 10 days for human HEV-infected cells), while β-actin was detected at equal levels in cells transfected with either siTsg101, siAlix, siNedd4 or siNc in both rat HEV-inoculated cells (Fig. 8B left, middle and right panel, respectively) and human HEV-inoculated cells (Fig. 8C left, middle and right panel respectively). The rat HEV RNA levels gradually increased and reached 2.3×10^6 copies/ml at 12 dpi in cells transfected with siNc. In contrast, the rat HEV RNA levels in Tsg101-depleted or Alix-depleted cells were only 8.3% (2.1×10^5 copies/ml) and 31.5% (6.7×10^5 copies/ml), respectively, compared to that of siNc at 12 dpi ($p < 0.001$, Fig. 8D). Similarly, specific depletion of Tsg101 or Alix significantly decreased the human HEV release to an average of 12.8% (1.3×10^4 copies/ml, $p < 0.001$) and 30.9% (3.2×10^4 copies/ml, $p < 0.01$), respectively, compared to that of siNc (1.0×10^5 copies/ml) at 10 dpi (Fig. 8E). These results

indicated that Tsg101 is important for rat HEV release; and that Alix is necessary for the release of both rat HEV and human HEV. However, the release of both rat HEV and human HEV in Nedd4-depleted cells increased to an average of 507.9% (1.2×10^7 copies/ml, Fig. 8F) and 436.3% (4.5×10^5 copies/ml, Fig. 8G), respectively ($p < 0.01$), compared to that of siNc from respective experiments.

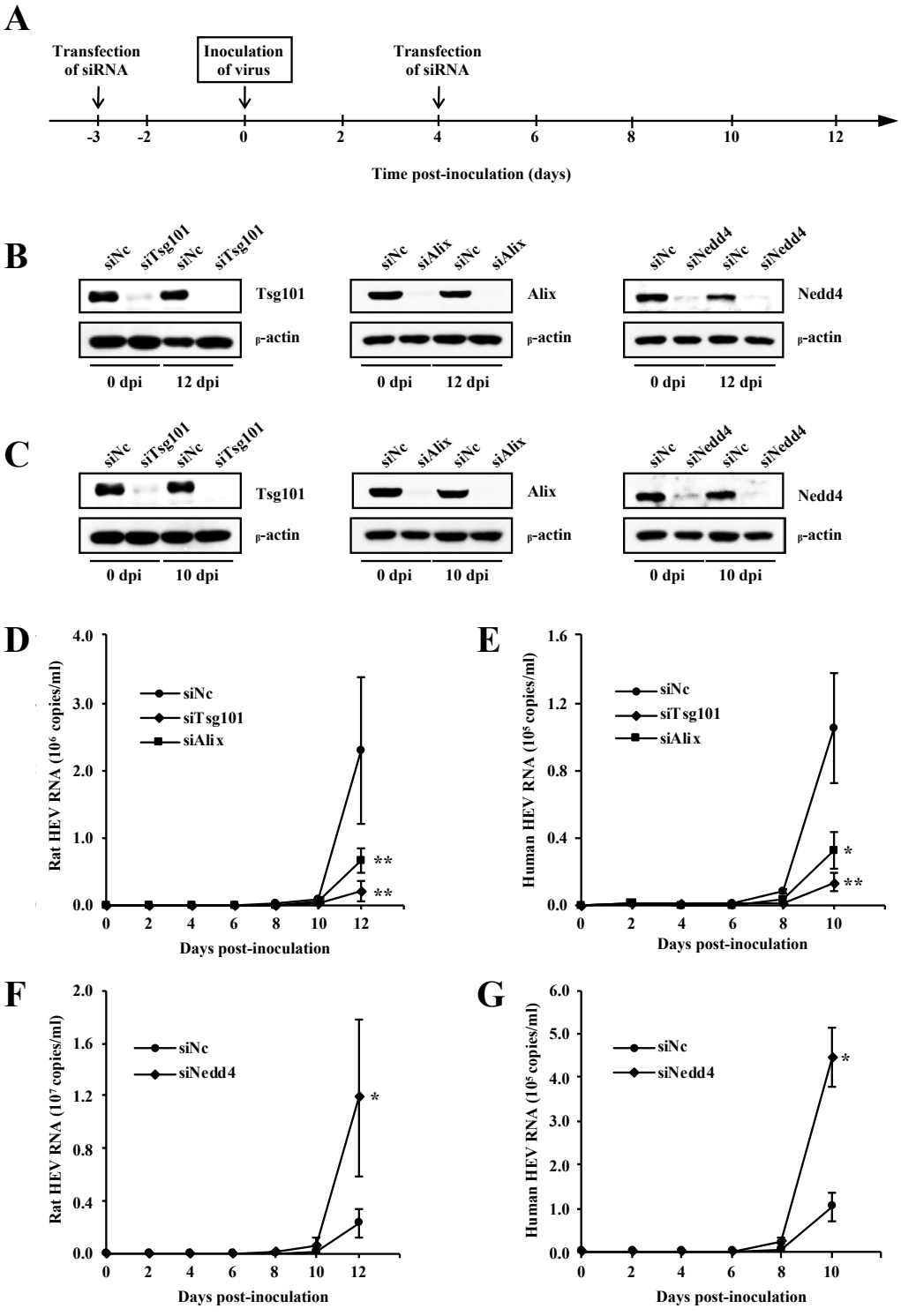

Fig. 8. Effects of siRNAs of Tsg101, Alix or Nedd4 on the release of rat HEV and human HEV. (A) Experiment schedule of siRNA assays. PLC/PRF/5 cells were transfected with siRNA both 3 days before and 4 days after virus inoculation on day 0. (B, C) The knock-down efficiency of siRNA in the experiments using rat HEV (B) and human HEV (C). On the indicated days after inoculation, cells were lysed and the expression of Tsg101 (left panel),

Alix (middle panel), Nedd4 (right panel) and β-actin were analyzed by Western blotting using anti-Tsg101 mAb, anti-Alix pAb, anti-Nedd4 pAb and anti-β-actin mAb, respectively. (D, E) The levels of extracellular rat HEV RNA (D) or human HEV RNA (E) in the cells treated with siTsg101 or siAlix compared to those of siNc. (F, G) The levels of extracellular rat HEV RNA (F) or human HEV RNA (G) in the cells treated with siNedd4, compared to those of siNc. The titer of rat HEV RNA or human HEV RNA titer was quantitated by real-time RT-PCR. All experiments were done in triplicate and the data represent the mean ± SD. *$p < 0.01$, **$p < 0.001$.

3.4. Effects of the overexpression of DN mutant of Nedd4

To confirm the results from the experiment using siNedd4, a DN mutant of Nedd4 was used. WW domains in Nedd4 were reported to be essential for binding to the PPxY motif in the viral L-domain. An Nedd4 mutant containing only the WW domains (Nedd4-WW) was known to inhibit virus budding in a DN manner [49]. Two days before inoculation, PLC/PRF/5 cells were transfected with 0.5 μg of empty vector or expression plasmid for Nedd4-WW. Transfection was then performed at 2, 6 and 10 dpi (Fig. 7A). Two days after the first transfection, the pretreated cells were inoculated with 1×10^6 copies/ml of cell culture-derived rat HEV or 2×10^5 copies/ml of cell culture-derived human HEV. The expression of Nedd4-WW in the experiment with rat HEV (Fig. 9A) and human HEV (Fig. 9B) was maintained during the observation period (12 days for rat HEV and 10 days for human HEV). The RNA levels of rat HEV (Fig. 9C) at 12 dpi in cells transfected with Nedd4-WW (2.8×10^5 copies/ml) did not differ markedly from that of empty vector (2.2×10^5 copies/ml) (78.1%, $p = 0.07$). Similarly, the RNA levels of human HEV (Fig. 9D) at 10 dpi (1.5×10^5 copies/ml) in cells transfected with Nedd4-WW did not differ markedly from

that of empty vector (1.4×10^5 copies/ml) (87.4%, $p = 0.29$). These results indicated that Nedd4 is not essential for the release of both rat HEV and human HEV.

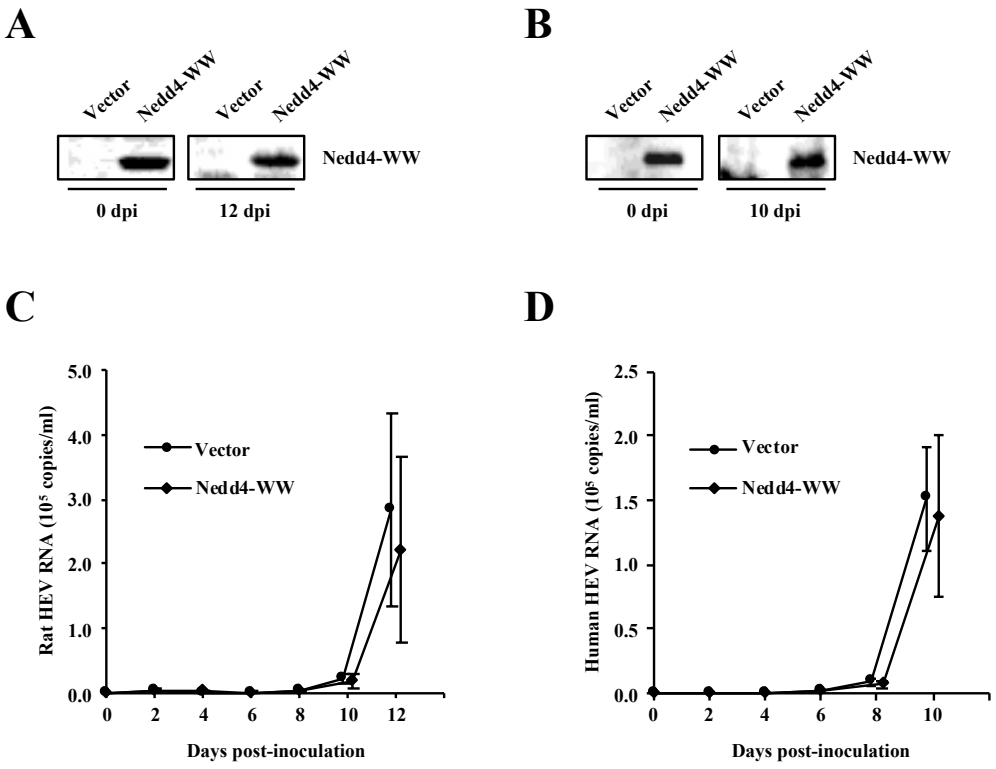

Fig. 9. Effects of DN mutant of Nedd4 on the release of rat HEV and human HEV. (A, B) The expression of DN mutant of Nedd4 in the experiment using rat HEV (A) or human HEV (B). PLC/PRF/5 cells were transfected with DN mutant of Nedd4 or empty vector. On the indicated days after inoculation, the cells were lysed, and the FLAG-tagged DN mutant of Nedd4 or empty vector was subjected to Western blotting with anti-FLAG pAb. (C, D) The levels of extracellular rat HEV RNA (C) or human HEV RNA (D) in cells transfected with the DN mutant of Nedd4, compared to those of empty vector. The titer of rat HEV RNA or human HEV RNA titer was quantitated by real-time RT-PCR. The data represent the mean ± SD of three independent experiments.

3.5. Requirement of the exosomal pathway for rat HEV release

To analyze the functional involvement of the exosomal pathway in rat HEV release, siRNAs targeting either Rab27A (siRab27A) or Hrs (siHrs) were used. Both were previously reported to be essential for the secretion of exosomes [53,54].

First, to confirm the co-localization of rat HEV ORF3 protein with Rab27A or Hrs in rat HEV-infected PLC/PRF/5 cells, double immunofluorescence staining was performed. The rat HEV ORF3 was co-localized with either Rab27A (Fig. 10A) or Hrs (Fig. 10B), indicating that both Rab27A and Hrs are associated with rat HEV replication. To deplete Rab27A or Hrs in PLC/PRF/5 cells, the cells were transfected with siRab27A, siHrs or siNc 3 days before and 4 days after virus inoculation (Fig. 8A). The depletion of Rab27A or Hrs in PLC/PRF/5 cells continued throughout the observation period, while no discernible alteration was observed in the expression level of β-actin (Fig. 10C). Three days after the first transfection, treated cells were inoculated with 1×10^6 copies/ml of cell culture-derived rat HEV. The rat HEV RNA levels increased gradually in the siNc-transfected cells, reaching 2.3×10^6 copies/ml at 12 dpi. In contrast, at 12 dpi, rat HEV release in Rab27A- or Hrs-depleted cells was significantly decreased to an average of 20.1% (5.3×10^5 copies/ml) and 18.5% (4.9×10^5 copies/ml), respectively ($p < 0.001$), compared to that of siNc (Fig. 10D). These results indicated that Rab27A and Hrs are important for rat HEV egress.

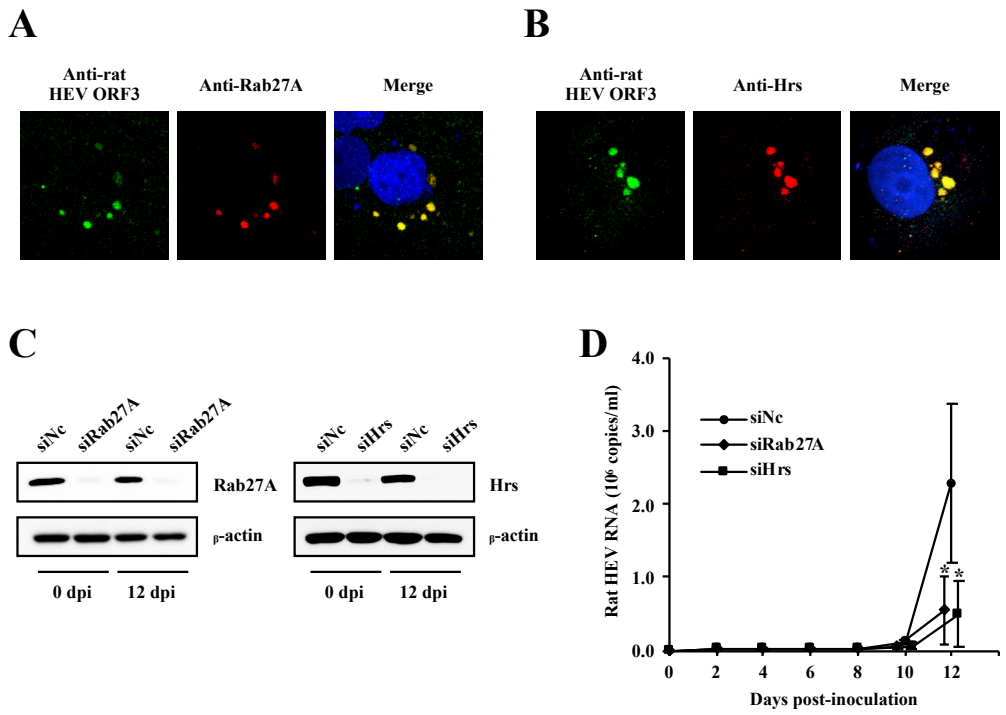

Fig. 10. Effects of siRNAs targeting Rab27A and Hrs on rat HEV release. (A, B) Results of the IFA. (A) Rat HEV-infected PLC/PRF/5 cells were incubated with anti-rat HEV ORF3 rabbit pAb (JB761) and anti-Rab27A mouse mAb, and subsequently stained with Alexa Fluor 488-conjugated anti-rabbit IgG and Alexa Fluor 594-conjugated mouse IgG. (B) Rat HEV-infected PLC/PRF/cells were incubated with anti-rat HEV ORF3 rabbit pAb (JB761) and anti-Hrs mouse mAb and subsequently stained with Alexa Fluor 488-conjugated anti-rabbit IgG and Alexa Fluor 594-conjugated mouse IgG. Co-localization is shown in yellow. The nuclei were stained with DAPI. Results representative of one of two experiments are shown. (C) The knock-down efficiency of siRNA. PLC/PRF/5 cells were treated with siRNA targeting Rab27A (siRab27A, left panel) or Hrs (siHrs, right panel), or negative control siNc. On the indicated days after inoculation, cells were lysed and the expression of Rab27A, Hrs or β-actin were analyzed by Western blotting using anti-Rab27A, anti-Hrs and anti-β-actin mAbs, respectively. (D) Levels of extracellular rat HEV RNA in cells treated with siRab27A or siHrs, compared to those of siNc. The rat HEV RNA titer was quantitated by real-time RT-PCR. All experiments were done in triplicate and the data represent the mean ± SD. *$p < 0.001$.

To support this finding, the involvement of the exosomal pathway in rat HEV release was examined by treating rat HEV-infected cells with either accelerator (Baf-A1) or inhibitor (GW4869) of exosome release. Baf-A1 is a vacuolar H^+-ATPase inhibitor that inhibits the lysosomal function [55], while GW4869 is a neutral sphingomyelinase inhibitor that inhibits ceramide biosynthesis [56]. Rat HEV-infected cells were treated with Baf-A1 or GW4869 for 24 h, and then the cells and their culture supernatants were collected. The extracellular rat HEV RNA levels were increased to 123.4%, 134.0%, 153.4% and 144.0% of the levels of the 1% DMSO-treated control after treatment for 24 h with 5, 10, 20 and 50 nM Baf-A1, respectively ($p < 0.01$, Fig. 11A), while the intracellular levels of rat HEV RNA were reduced to 96.5%, 90.2%, 82.1% and 76.1% of the 1% DMSO-treated control after treatment with 5, 10, 20 and 50 nM Baf-A1, respectively ($p < 0.05$ or $p < 0.01$, Fig. 11B). These results suggested that the rat HEV release was accelerated by Baf-A1. The extracellular rat HEV RNA levels were decreased to 94.3%, 81.3%, 64.9% and 55.5% of the levels of the 1% DMSO-treated control after treatment for 24 h with 2, 5, 20 and 50 μM GW4869, respectively ($p < 0.05$ or $p < 0.001$, Fig. 11C). In contrast, the intracellular rat HEV RNA levels were increased to 108.1%, 112.3%, 118.6% and 134.2% after treatment with 2, 5, 20 and 50 μM GW4869, respectively ($p < 0.05$, $p < 0.01$ or $p < 0.001$, Fig. 11D), suggesting that GW4869 inhibited rat HEV release without affecting the replication of rat HEV RNA. The MTS assay showed that the two drugs did not significantly affect the viability or survival of the cells within 24 h of application (Fig. 11E). Taken together, these results indicated that rat HEV utilizes the exosomal pathway for its egress from infected cells.

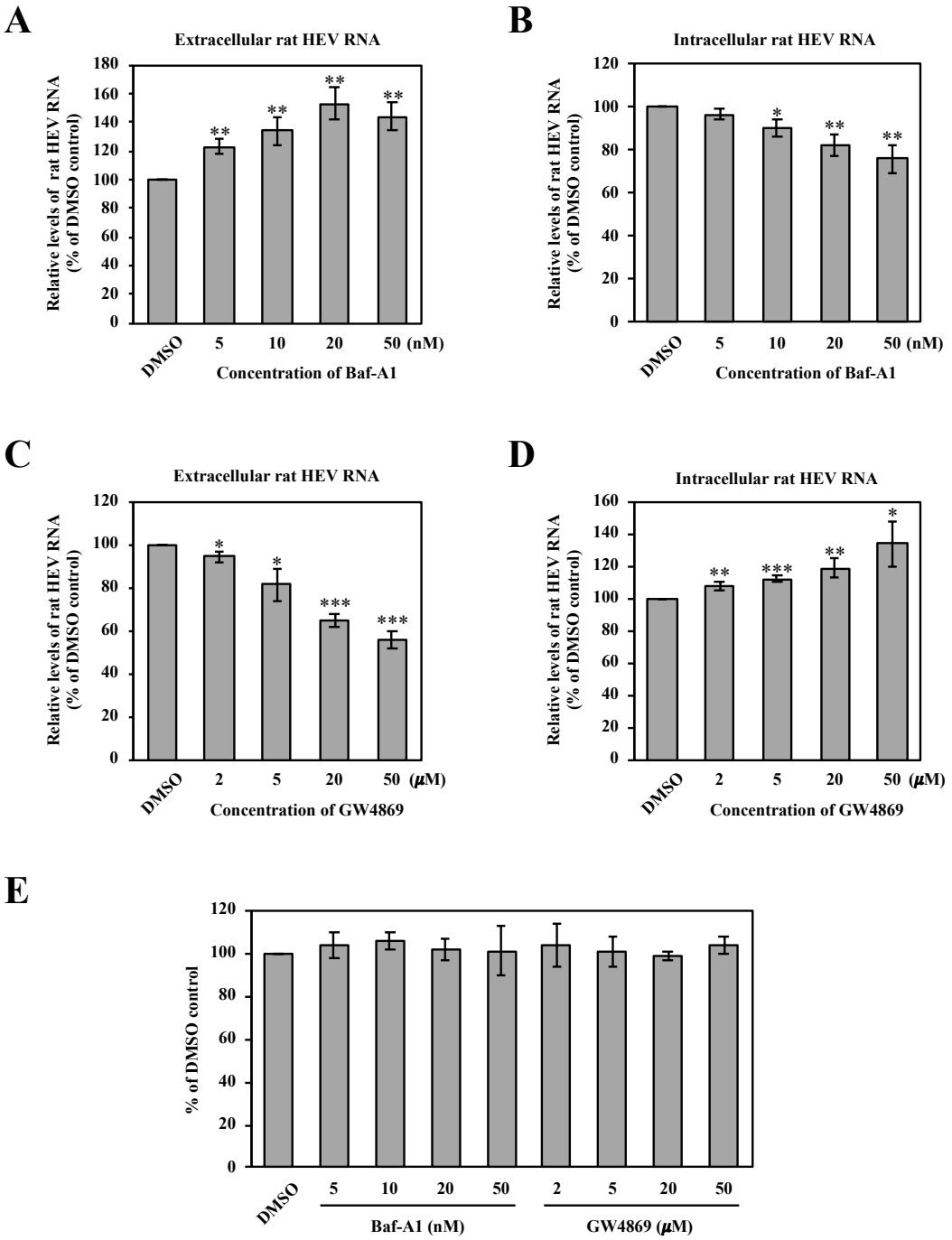

Fig. 11. Effects of accelerator or inhibitor of exosome release on rat HEV release. The rat HEV-infected PLC/PRF/5 cells were cultivated with growth medium containing 0 to 50 nM Baf-A1 in the presence of 1% DMSO or 0 to 50 μM GW4869 in the presence of 1% DMSO for 24 h. (A, B) The levels of extracellular (A) and intracellular (B) rat HEV RNA in the rat HEV-infected cells treated with Baf-A1. (C, D) The levels of extracellular (C) and intracellular (D) rat HEV RNA in the infected cells treated with GW4869. (E) The analysis

of the cellular proliferation and survival by the MTS assay. The rat HEV RNA titer was quantitated by real-time RT-PCR. All experiments were done in duplicate and the data represent the mean ± SD. *$p < 0.05$, **$p < 0.01$, ***$p < 0.001$.

3.6. Intracellular co-localization of rat HEV proteins with MVB and exosomal protein markers

The presence of membrane-associated HEV particles with the membrane having exosome-specific molecules has been reported previously [38]. The present study revealed that Tsg101 and Alix were important for rat HEV egress from infected cells. These proteins are not only components of the ESCRT machinery but also exosomal marker proteins. To confirm whether or not these marker proteins are co-localized with rat HEV ORF3 protein, IFA was performed. Rat HEV ORF3 was co-localized with either Tsg101 or Alix in the cytoplasm as shown by double immunofluorescence staining (Figs. 12A and B, respectively). These observations further support the findings of the present study that rat HEV utilizes MVB sorting and exosomal pathway for its egress.

Next, the co-localization of rat HEV ORF2 and rat HEV ORF3 proteins with CD63 was examined. A previous study demonstrated that human HEV ORF2 and ORF3 proteins were co-localized with CD63 (an MVB and exosome marker protein) in infected cells, and that IEM showed positive immunogold staining for human HEV ORF2 on the intraluminal vesicles within the MVB [40]. Double immunofluorescence staining revealed that CD63 was co-localized with rat HEV ORF2 (Fig. 12C) or rat HEV ORF3 (Fig. 12D) proteins in the cytoplasm. Furthermore, triple staining showed that the three proteins were partially co-localized in the cytoplasm with specific

loculated signals (Fig. 12E). These results suggested that membrane-associated rat HEV particles are present within the MVB.

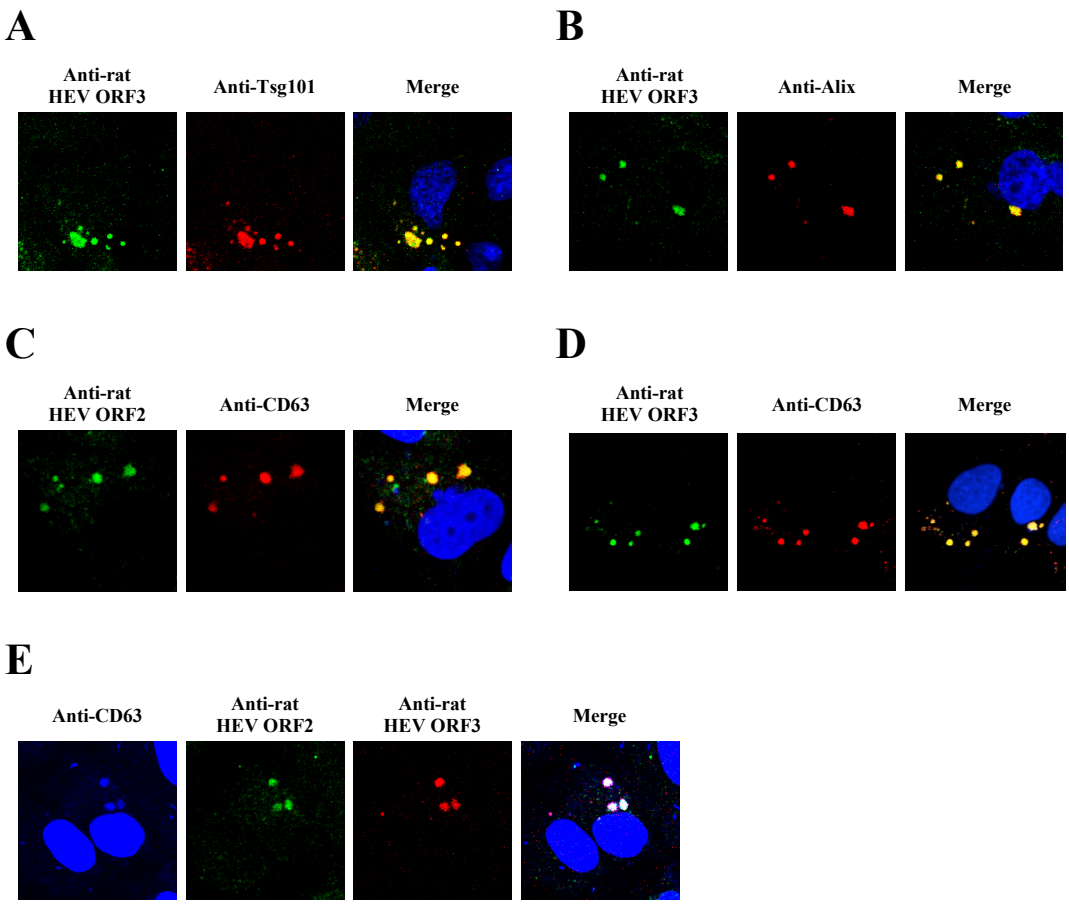

Fig. 12. Intracellular co-localization of rat HEV proteins with MVB and exosomal protein markers. (A) Rat HEV-infected PLC/PRF/5 cells were incubated with anti-rat HEV ORF3 rabbit pAb (JB761) and anti-Tsg101 mouse mAb and then stained with Alexa Fluor 488-conjugated anti-rabbit IgG and Alexa Fluor 594-conjugated anti-mouse IgG. (B) Rat HEV-infected PLC/PRF/5 cells were incubated with anti-rat HEV ORF3 mouse mAb (TA7126) and anti-Alix rabbit pAb and then stained with Alexa Fluor 488-conjugated anti-mouse IgG and Alexa Fluor 594-conjugated anti-rabbit IgG. (C) Rat HEV-infected PLC/PRF/5 cells were incubated with anti-rat HEV ORF2 mouse mAb (TA7005) and anti-CD63 rabbit pAb and then stained with Alexa Fluor 488-conjugated anti-mouse IgG and Alexa Fluor 594-conjugated anti-rabbit IgG. (D) Rat HEV-infected PLC/PRF/5 cells were incubated with anti-rat HEV ORF3 rabbit pAb (JB761) and anti-CD63 goat pAb and then

stained with Alexa Fluor 488-conjugated anti-rabbit IgG and Alexa Fluor 555-conjugated anti-goat IgG. (E) Triple immunofluorescent staining of rat HEV-infected PLC/PRF/5 cells incubated with anti-rat HEV ORF2 mouse mAb (TA7005), anti-rat HEV ORF3 rabbit pAb (JB761) and anti-CD63 goat pAb and then stained with Alexa Fluor 488-conjugated anti-mouse IgG, Alexa Fluor 594-conjugated anti-rabbit IgG and Alexa Fluor 350-conjugated anti-goat IgG. Co-localization of double or triple staining is shown in yellow or white, respectively. The nuclei were stained with DAPI. Images are representative of one of two experiments.

3.7. Interaction of rat HEV ORF3 with host cellular factors Tsg101, Alix or Nedd4

It was previously demonstrated that human HEV ORF3 protein interacts with Tsg101 via its PSAP motif to support virion release from infected cells [5,39]. In the present study, depletion of Tsg101 or Alix significantly decreased the release of rat HEV (Fig. 8D). In addition, depletion of Tsg101 or Alix significantly decreased the release of human HEV (Fig. 8E). In contrast, the overexpression of DN mutant of Nedd4 did not affect the release of rat or human HEV (Figs. 9C and D, respectively).

An IP assay was performed to examine whether or not rat HEV ORF3 protein directly interacts with the host cellular factors Tsg101, Alix or Nedd4, compared with human HEV ORF3 protein. PLC/PRF/5 cells were transfected with expression plasmid encoding rat or human HEV ORF3 protein. The extracts of the transfected cells were then immunoprecipitated with either anti-Tsg101 pAb, anti-Alix pAb, anti-Nedd4 pAb, anti-rat HEV ORF3 pAb or anti-human HEV ORF3 mAb. The immunoprecipitates were then subjected to Western blotting using either anti-rat HEV ORF3 pAb or anti-human HEV ORF3 mAb. Cell extracts expressing rat HEV ORF3 protein were not co-immunoprecipitated with anti-Tsg101 pAb (Fig. 13A), in contrast to the cell extracts expressing human HEV ORF3 protein that were co-immunoprecipitated with anti-Tsg101 pAb (Fig. 13B). These results indicated that

unlike human HEV ORF3 protein, rat HEV ORF3 protein does not interact with Tsg101.

In addition, IP assays with anti-Alix or anti-Nedd4 pAb for cell extracts expressing rat or human HEV ORF3 protein were not detected by Western blotting with anti-rat HEV ORF3 (Fig. 13A) or anti-human HEV ORF3 (Fig. 13B), respectively, indicating that neither rat HEV ORF3 nor human HEV ORF3 protein interacts with Alix nor Nedd4. Cell extracts expressing rat or human HEV ORF3 protein were immunoprecipitated with anti-rat HEV ORF3 pAb (Fig. 13A) or human HEV ORF3 mAb (Fig. 13B), respectively, indicating the specificity of this assay.

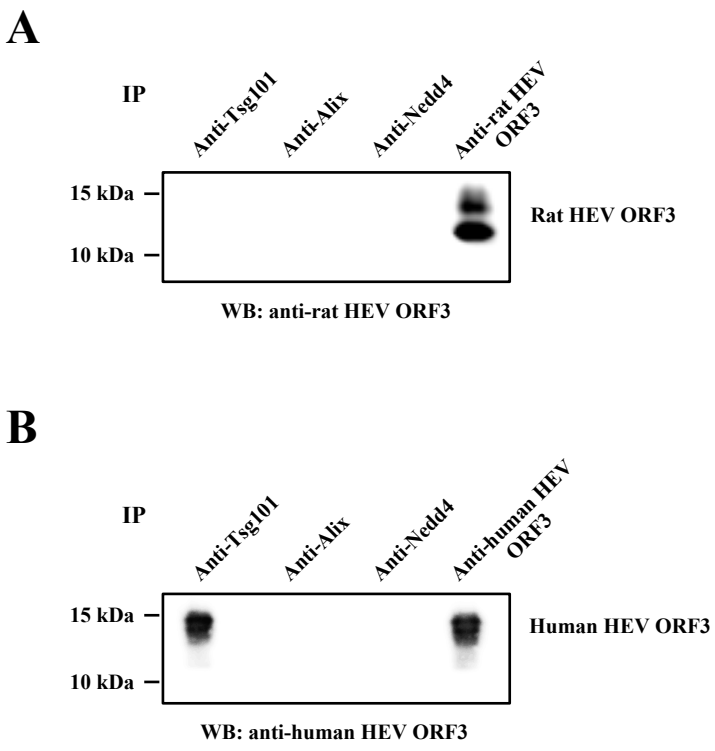

Fig. 13. Interaction of HEV ORF3 protein with host factors. PLC/PRF/5 cells were transfected with rat HEV ORF3 protein or human HEV ORF3 protein. The cell lysates were immunoprecipitated with either anti-Tsg101, anti-Alix or anti-Nedd4, in comparison with anti-rat HEV ORF3 pAb (A) or anti-human HEV ORF3 mAb (B). The immunoprecipitates

were then subjected to Western blotting with either anti-rat HEV ORF3 pAb (A) or anti-human HEV ORF3 mAb (B). Results are representative of two experiments.

3.8. Host cellular proteins that bind to rat HEV ORF3 protein

It was previously reported that cells transfected with mutated rat HEV RNA harboring three amino acids substitutions (aa 93, 96 and 98) in the proline-rich region of rat HEV ORF3 protein showed membrane disruption, thus inhibiting virus release [43]. As Tsg101 does not interact with rat HEV ORF3 protein (despite its association with rat HEV release), the host cellular factors that might bind to rat HEV ORF3 protein were examined by performing a co-IP assay followed by silver staining.

First, FLAG- or Myc-tagged wild-type rat HEV ORF3 protein and its mutant were constructed. The rat HEV ORF3 mutant has three amino acids mutated from proline into leucine in the proline-rich region of the ORF3 (aa 93, 96 and 98) (Fig. 14A). In the current experiment, PLC/PRF/5 cells transfected with FLAG- or Myc-tagged wild-type or its mutant, or empty vector as a comparison, were extracted, and the expression was confirmed by Western blotting using either anti-rat HEV ORF3 pAb and anti-FLAG mAb (Fig. 14B, left panel) or anti-rat HEV ORF3 pAb and anti-Myc mAb (Fig. 14B, right panel).

Subsequently, cells were transfected with either FLAG- or Myc-tagged wild-type or its mutant, or empty vector. The extracts were immunoprecipitated with either anti-FLAG or anti-Myc mAb. The immunoprecipitates were subjected to gel electrophoresis and subsequently to silver staining. A host cellular protein at an approximate size of 90 kDa was seen to bind to either FLAG- or Myc-tagged wild-type rat HEV ORF3 but not to the mutants or the empty vectors (Fig. 14C). When a

similar experiment was performed using human HEV ORF3 protein, there was no host protein detected at the approximate size of 90 kDa (data not shown). These results indicate that the 90 kDa protein can bind specifically to wild-type rat HEV ORF3.

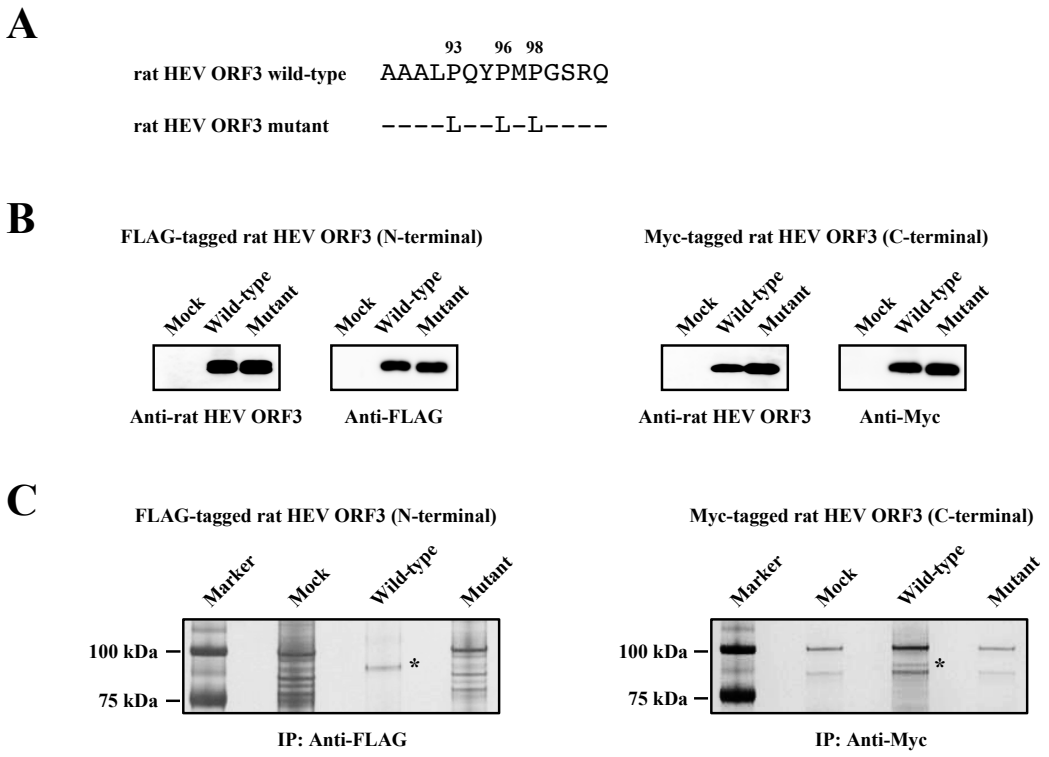

Fig. 14. Host cellular proteins that bind to rat HEV ORF3 protein. (A) A FLAG- or Myc-tagged wild-type or mutant rat HEV ORF3 protein was constructed. The mutant rat HEV ORF3 protein has three amino acids mutations from proline (P) into leucine (L) at aa 93, 96 and 98. (B) PLC/PRF/5 cells were transfected with FLAG- (left panel) or Myc-tagged (right panel) wild-type or its mutant. The cell lysates were subjected to Western blotting using anti-rat HEV ORF3 pAb and anti-FLAG mAb (left panel) or anti-rat HEV pAb and anti-Myc mAb (right panel). (C) PLC/PRF/5 cells were transfected with FLAG- (left panel) or Myc-tagged (right panel) wild-type or its mutant. Cell lysates were immunoprecipitated with anti-FLAG (left panel) and anti-Myc (right panel) mAbs. The immunoprecipitates were subjected to gel electrophoresis and silver staining. Results are representative of one of three experiments. The asterisk (*) indicates the host protein (approximately 90 kDa) bound to rat HEV ORF3 protein.

4. Discussion

A previous study revealed that the release of rat HEV from infected cells is associated with ORF3 protein, especially its PxYPMP motif (PQYPMP in the aforementioned study) [43]; however, the mechanism underlying the virion release remains elusive. This question was addressed in the present study by analyzing the release mechanism of rat HEV related to the utilization of MVB sorting and the exosomal pathway, as these have been shown to be used by human HEV for virion egress [39,40].

My present morphological analysis by TEM revealed that rat HEV particles are membrane-associated in culture supernatants (Fig. 6A) and became membrane-unassociated particles of a smaller size after treatment with detergent and protease to remove the membranes (Fig. 6B). This is in agreement with the findings in human HEV [38], and suggests that the capsids of rat HEV particles are individually covered by a lipid membrane.

Many enveloped viruses acquire their membrane by hijacking the host cells' ESCRT machinery to facilitate the final stages of virion release, such as for HIV [57] and Ebola virus [49]. Outside of enveloped viruses, quasi-enveloped viruses, such as hepatitis A virus (HAV), were recently reported to also use the ESCRT machinery for their release [30]. In human HEV and avian HEV, the ESCRT components or ESCRT-related components involved in this event are Tsg101, Vps4A and Vps4B [39,58]. In the present study, rat HEV release was revealed to be ESCRT-dependent, as the overexpression of DN mutants of Vps4A or Vps4B inhibited the rat HEV release (Fig. 7D), and the depletion of endogenous Tsg101 reduced the release efficiency of rat

HEV (Fig. 8D). I also found that depletion of endogenous Alix decreased the virus release of not only rat HEV (Fig. 8D) but human HEV as well (Fig. 8E). These results support the notion that the release of rat HEV is ESCRT-dependent with components such as Tsg101, Alix and Vps4A/B. In addition, rat HEV ORF3 protein was co-localized with either Tsg101 (Fig. 12A) or Alix (Fig. 12B), further supporting the notion that these two ESCRT components are associated with rat HEV release.

However, another ESCRT-related component Nedd4 was not found to be essential for the release of rat HEV (Fig. 9C) or human HEV (Fig. 9D), as suggested by the overexpression of its DN mutant, which did not affect the release efficiency. This finding is consistent with the statement that budding does not depend on all components of the canonical ESCRT pathway [59]; for example, HIV-1 recruits Tsg101 and/or Alix and requires a subset of ESCRT-III proteins together with Vps4A/B, while the ESCRT-0, ESCRT-II and several ESCRT-III proteins are expendable [60]. In contrast, herpes simplex virus-1 (HSV-1) budding depends on a smaller subset of the ESCRT machinery, only requiring a functional ESCRT-III complex but no Tsg101 or Alix [61]. Murine leukemia virus (MLV) (subviral and viral particle), has also been reported to require only a small subset of ESCRT components [ESCRT-I component Tsg101 and ESCRT-III components (CHMP2A and CHMP4B)], together with supportive roles played by the ESCRT/MVB-associated factors Alix and Nedd4-1 [27].

A previous study showed the triple co-localization of CD63 (MVB and exosome marker protein) with human HEV ORF2 and ORF3 by IFA, with the co-localization further supported by TEM images indicating that membrane-associated particles were present within MVB [40]. In rat HEV, the co-localization of either rat HEV ORF2 (Fig. 12C) or ORF3 (Fig. 12D) with CD63 or their triple co-localization (Fig. 12E)

supported the notion that membrane-associated rat HEV particles are also present within MVB in infected cells.

The membrane-associated HEV and HAV particles resemble exosomes, as they share a common mechanism of biogenesis involving secretion through the MVB pathway [30,38,40]. To study the utilization of the exosomal pathway by rat HEV for its release, siRNA targeting Rab27A or Hrs, which are components required for exosomal secretion, was used. The rat HEV release was indeed inhibited by the depletion of endogenous Rab27A or Hrs (Fig. 10D). In addition, rat HEV ORF3 protein was co-localized with either Rab27A or Hrs (Figs. 10A, B). I also showed that treatment of rat HEV-infected cells with Baf-A1, an accelerator of exosome secretion, significantly increased the extracellular rat HEV RNA in a dose-dependent manner (Fig. 11A), while treatment with GW4869 (an inhibitor of exosome secretion) decreased the extracellular rat HEV RNA (Fig. 11C), further supporting the notion that rat HEV utilizes the exosomal pathway for its egress, similar to other viruses, such as hepatitis C virus (HCV) [54,62] and human herpes virus 6 (HHV-6) [63].

Taken together, the present findings indicated that rat HEV utilizes MVB sorting and the exosomal pathway to support its egress from infected cells. Rat HEV virions bud into the MVB, which promotes membrane formation. Upon fusion of the MVB membrane and the plasma membrane, the quasi-enveloped virions are then released together with internal vesicles through the exosomal pathway, which is regulated by Rab27 and Hrs.

The results from siRNA assays and IFA indicated that both Tsg101 and Alix are associated with rat HEV egress. However, rat HEV ORF3 did not bind to either protein (Fig. 13A). It was previously reported that rat HEV has a proline-rich sequence (PxYPMP) that is well-conserved among *Orthohepevirus C* species including

genotypes C1 (from rats) and C2 (from ferrets). This motif was suggested to be associated with rat HEV egress in the aforementioned study, where the substitution of leucine for proline in the PQYPMP motif of rat HEV ORF3 into LQYLML was associated with disrupted membrane formation, and thus decreased virus release [43]. In the present study, this rat HEV ORF3 mutant was used (Fig. 14A) to confirm that the possible host factor can bind to the specific motif. The present analysis using the expressed rat HEV ORF3 protein tagged with FLAG (N-terminal) or Myc (C-terminal) (Fig. 14B) suggested that one host cellular protein at an approximate size of 90 kDa was bound to either FLAG- or Myc-tagged rat HEV ORF3 wild-type (Fig. 14C). Interestingly, this host protein did not bind to either rat HEV ORF3 mutant (Fig. 14C). As this protein bound only to the rat HEV ORF3 wild-type, it might be a candidate alternative to Tsg101, which is known to bind to the ESCRT-related motif in human and avian HEV ORF3, PSAP.

5. Conclusions

Fig. 15 summarizes the results of this study. In the present study, I showed that rat HEV utilizes MVB sorting and the exosomal pathway to support its egress from infected cells. While the results from siRNA assays and IFA indicated that both Tsg101 and Alix are associated with rat HEV release, rat HEV ORF3 did not bind to either protein. I detected one host cellular protein at an approximate size of 90 kDa that bound to wild-type rat HEV ORF3 (but not to its mutant with proline to leucine mutations in the PxYPMP motif) and might be a possible candidate alternative to Tsg101, associated with virion egress (or with other ORF3-related functions). The exploration of host cellular factors that bind to rat HEV ORF3 to support virion egress warrants further study.

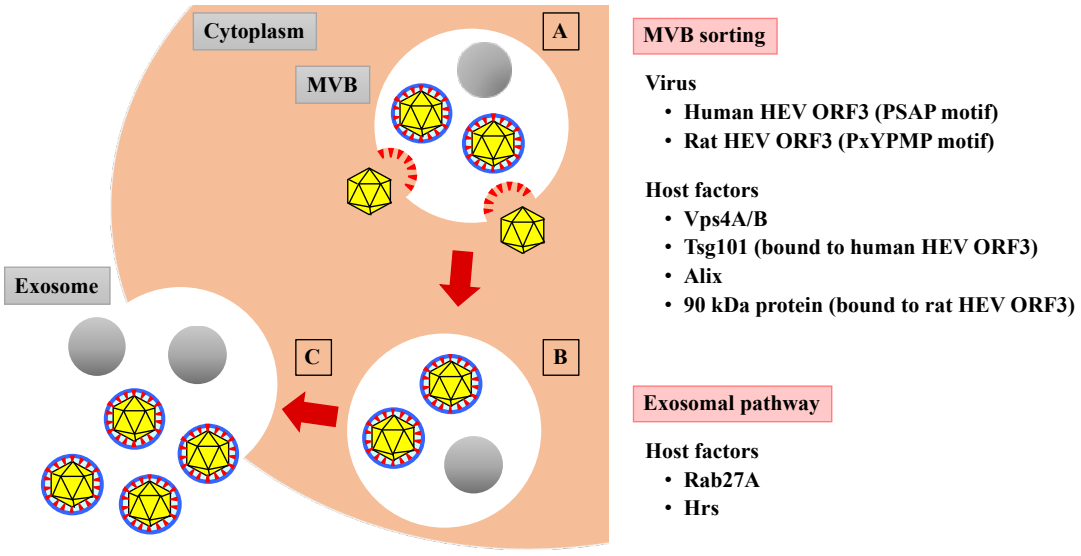

Fig. 15. Mechanism of rat and human HEV egress from infected cells. (A) HEV buds endosomal membrane by MVB sorting. (B) The membrane-associated HEV particles are present in the MVB within internal vesicles. (C) HEV particles are released together with internal vesicles by the cellular exosomal pathway.

Conflicts of Interest

I declare that there are no conflicts of interest.

Acknowledgements

I am grateful to Dr. Tom Kouki (Jichi Medical University) for his excellent technical assistance and critical comments regarding EM and to Prof. Jiro Yasuda (Nagasaki University) for providing the plasmids: FLAG-tagged Vps4 (pVps4A, pVps4B and DN mutants) and DN mutant of Nedd4 (pNedd4.1-WW).

This study was supported in part by Jichi Medical University Graduate Student Research Award and the Research Program on Hepatitis from the Japan Agency for Medical Research and Development, AMED (JP19fk0210043 to Prof. Hiroaki Okamoto, Jichi Medical University).

References

1. Primadharsini, P. P., Nagashima, S. & Okamoto, H. Genetic variability and evolution of hepatitis E virus. *Viruses* **11**, 456, 2019.
2. Koonin, E. V., Gorbalenya, A. E., Purdy, M. A., Rozanov, M. N., Reyes, G. R. & Bradley, D. W. Computer-assisted assignment of functional domains in the nonstructural polyprotein of hepatitis E virus: delineation of an additional group of positive-strand RNA plant and animal viruses. *Proc Natl Acad Sci U S A* **89**, 8259-8263, 1992.
3. Reyes, G. R., Huang, C. C., Tam, A. W. & Purdy, M. A. Molecular organization and replication of hepatitis E virus (HEV). *Arch Virol Suppl* **7**, 15-25, 1993.
4. Yamada, K., Takahashi, M., Hoshino, Y., Takahashi, H., Ichiyama, K., Nagashima, S., Tanaka, T. & Okamoto, H. ORF3 protein of hepatitis E virus is essential for virion release from infected cells. *J Gen Virol* **90**, 1880-1891, 2009.
5. Nagashima, S., Takahashi, M., Jirintai, Tanaka, T., Yamada, K., Nishizawa, T. & Okamoto, H. A PSAP motif in the ORF3 protein of hepatitis E virus is necessary for virion release from infected cells. *J Gen Virol* **92**, 269-278, 2011.
6. Ding, Q., Heller, B., Capuccino, J. M., Song, B., Nimgaonkar, I., Hrebikova, G., Contreras, J. E. & Ploss, A. Hepatitis E virus ORF3 is a functional ion channel required for release of infectious particles. *Proc Natl Acad Sci U S A* **114**, 1147-1152, 2017.
7. Purdy, M. A., Harrison, T. J., Jameel, S., Meng, X. J., Okamoto, H., Van der Poel, W. H. M., Smith, D. B. & ICTV Report, C. ICTV Virus Taxonomy Profile: Hepeviridae. *J Gen Virol* **98**, 2645-2646, 2017.
8. Tam, A. W., Smith, M. M., Guerra, M. E., Huang, C. C., Bradley, D. W., Fry, K. E. & Reyes, G. R. Hepatitis E virus (HEV): molecular cloning and sequencing of the full-length viral genome. *Virology* **185**, 120-131, 1991.
9. Kabrane-Lazizi, Y., Meng, X. J., Purcell, R. H. & Emerson, S. U. Evidence that the genomic RNA of hepatitis E virus is capped. *J Virol* **73**, 8848-8850, 1999.

10. WHO. Hepatitis E. <https://www.who.int/news-room/fact-sheets/detail/hepatitis-E> (2019).
11. IDWR. IDWR surveillance data table 2019. <https://www.niid.go.jp/niid/en/data.html> (2019).
12. Perez-Gracia, M. T., Suay-Garcia, B. & Mateos-Lindemann, M. L. Hepatitis E and pregnancy: current state. *Rev Med Virol* **27**, e1929, 2017.
13. Kamar, N., Selves, J., Mansuy, J. M., Ouezzani, L., Peron, J. M., Guitard, J., Cointault, O., Esposito, L., Abravanel, F., Danjoux, M., Durand, D., Vinel, J. P., Izopet, J. & Rostaing, L. Hepatitis E virus and chronic hepatitis in organ-transplant recipients. *N Engl J Med* **358**, 811-817, 2008.
14. Shrestha, A., Adhikari, A., Bhattarai, M., Rauniyar, R., Debes, J. D., Boonstra, A., Lama, T. K., Al Mahtab, M., Butt, A. S., Akbar, S. M. F., Aryal, N., Karn, S., Manandhar, K. D. & Gupta, B. P. Prevalence and risk of hepatitis E virus infection in the HIV population of Nepal. *Virol J* **14**, 228, 2017.
15. Kamar, N., Marion, O., Abravanel, F., Izopet, J. & Dalton, H. R. Extrahepatic manifestations of hepatitis E virus. *Liver Int* **36**, 467-472, 2016.
16. Kumar, S., Stecher, G. & Tamura, K. MEGA7: molecular evolutionary genetics analysis version 7.0 for bigger datasets. *Mol Biol Evol* **33**, 1870-1874, 2016.
17. Okamoto, H. Genetic variability and evolution of hepatitis E virus. *Virus Res* **127**, 216-228, 2007.
18. Meng, X. J. Zoonotic and foodborne transmission of hepatitis E virus. *Semin Liver Dis* **33**, 41-49, 2013.
19. Kamar, N., Lhomme, S., Abravanel, F., Marion, O., Peron, J. M., Alric, L. & Izopet, J. Treatment of HEV infection in patients with a solid-organ transplant and chronic hepatitis. *Viruses* **8**, 222, 2016.
20. Satake, M., Matsubayashi, K., Hoshi, Y., Taira, R., Furui, Y., Kokudo, N., Akamatsu, N., Yoshizumi, T., Ohkohchi, N., Okamoto, H., Miyoshi, M., Tamura, A., Fuse, K. & Tadokoro, K. Unique clinical courses of transfusion-transmitted hepatitis E in patients with immunosuppression. *Transfusion* **57**, 280-288, 2017.
21. Kenney, S. P. The current host range of hepatitis E viruses. *Viruses* **11**, 452, 2019.

22. Lee, G. H., Tan, B. H., Teo, E. C., Lim, S. G., Dan, Y. Y., Wee, A., Aw, P. P., Zhu, Y., Hibberd, M. L., Tan, C. K., Purdy, M. A. & Teo, C. G. Chronic infection with camelid hepatitis E virus in a liver transplant recipient who regularly consumes camel meat and milk. *Gastroenterology* **150**, 355-357 e353, 2016.
23. Sridhar, S., Yip, C. C. Y., Wu, S., Cai, J., Zhang, A. J., Leung, K. H., Chung, T. W. H., Chan, J. F. W., Chan, W. M., Teng, J. L. L., Au-Yeung, R. K. H., Cheng, V. C. C., Chen, H., Lau, S. K. P., Woo, P. C. Y., Xia, N. S., Lo, C. M. & Yuen, K. Y. Rat hepatitis E virus as cause of persistent hepatitis after liver transplant. *Emerg Infect Dis* **24**, 2241-2250, 2018.
24. Andonov, A., Robbins, M., Borlang, J., Cao, J., Hatchette, T., Stueck, A., Deschambault, Y., Murnaghan, K., Varga, J. & Johnston, L. Rat Hepatitis E virus linked to severe acute hepatitis in an immunocompetent patient. *J Infect Dis* **220**, 951-955, 2019.
25. Bieniasz, P. D. Late budding domains and host proteins in enveloped virus release. *Virology* **344**, 55-63, 2006.
26. Kenney, S. P., Wentworth, J. L., Heffron, C. L. & Meng, X. J. Replacement of the hepatitis E virus ORF3 protein PxxP motif with heterologous late domain motifs affects virus release via interaction with Tsg101. *Virology* **486**, 198-208, 2015.
27. Bartusch, C. & Prange, R. ESCRT requirements for murine leukemia virus release. *Viruses* **8**, 103, 2016.
28. Ahmed, I., Akram, Z., Iqbal, H. M. N. & Munn, A. L. The regulation of endosomal sorting complex required for transport and accessory proteins in multivesicular body sorting and enveloped viral budding - an overview. *Int J Biol Macromol* **127**, 1-11, 2019.
29. Garrus, J. E., von Schwedler, U. K., Pornillos, O. W., Morham, S. G., Zavitz, K. H., Wang, H. E., Wettstein, D. A., Stray, K. M., Cote, M., Rich, R. L., Myszka, D. G. & Sundquist, W. I. Tsg101 and the vacuolar protein sorting pathway are essential for HIV-1 budding. *Cell* **107**, 55-65, 2001.
30. Feng, Z., Hensley, L., McKnight, K. L., Hu, F., Madden, V., Ping, L., Jeong, S. H., Walker, C., Lanford, R. E. & Lemon, S. M. A pathogenic picornavirus

acquires an envelope by hijacking cellular membranes. *Nature* **496**, 367-371, 2013.

31. Yasuda, J., Hunter, E., Nakao, M. & Shida, H. Functional involvement of a novel Nedd4-like ubiquitin ligase on retrovirus budding. *EMBO Rep* **3**, 636-640, 2002.
32. Votteler, J. & Sundquist, W. I. Virus budding and the ESCRT pathway. *Cell Host Microbe* **14**, 232-241, 2013.
33. van der Pol, E., Boing, A. N., Harrison, P., Sturk, A. & Nieuwland, R. Classification, functions, and clinical relevance of extracellular vesicles. *Pharmacol Rev* **64**, 676-705, 2012.
34. Robbins, P. D. & Morelli, A. E. Regulation of immune responses by extracellular vesicles. *Nat Rev Immunol* **14**, 195-208, 2014.
35. Anderson, M. R., Kashanchi, F. & Jacobson, S. Exosomes in viral disease. *Neurotherapeutics* **13**, 535-546, 2016.
36. Takahashi, M., Yamada, K., Hoshino, Y., Takahashi, H., Ichiyama, K., Tanaka, T. & Okamoto, H. Monoclonal antibodies raised against the ORF3 protein of hepatitis E virus (HEV) can capture HEV particles in culture supernatant and serum but not those in feces. *Arch Virol* **153**, 1703-1713, 2008.
37. Takahashi, M., Tanaka, T., Takahashi, H., Hoshino, Y., Nagashima, S., Jirintai, Mizuo, H., Yazaki, Y., Takagi, T., Azuma, M., Kusano, E., Isoda, N., Sugano, K. & Okamoto, H. Hepatitis E Virus (HEV) strains in serum samples can replicate efficiently in cultured cells despite the coexistence of HEV antibodies: characterization of HEV virions in blood circulation. *J Clin Microbiol* **48**, 1112-1125, 2010.
38. Nagashima, S., Takahashi, M., Kobayashi, T., Tanggis, Nishizawa, T., Nishiyama, T., Primadharsini, P. P. & Okamoto, H. Characterization of the quasi-enveloped hepatitis E virus particles released by the cellular exosomal pathway. *J Virol* **91**, e00822-17, 2017.
39. Nagashima, S., Takahashi, M., Jirintai, S., Tanaka, T., Nishizawa, T., Yasuda, J. & Okamoto, H. Tumour susceptibility gene 101 and the vacuolar protein sorting pathway are required for the release of hepatitis E virions. *J Gen Virol* **92**, 2838-2848, 2011.

40. Nagashima, S., Jirintai, S., Takahashi, M., Kobayashi, T., Tanggis, Nishizawa, T., Kouki, T., Yashiro, T. & Okamoto, H. Hepatitis E virus egress depends on the exosomal pathway, with secretory exosomes derived from multivesicular bodies. *J Gen Virol* **95**, 2166-2175, 2014.
41. Primadharsini, P. P., Mulyanto, Wibawa, I. D. N., Anggoro, J., Nishizawa, T., Takahashi, M., Jirintai, S. & Okamoto, H. The identification and characterization of novel rat hepatitis E virus strains in Bali and Sumbawa, Indonesia. *Arch Virol* **163**, 1345-1349, 2018.
42. Jirintai, S., Tanggis, Mulyanto, Suparyatmo, J. B., Takahashi, M., Kobayashi, T., Nagashima, S., Nishizawa, T. & Okamoto, H. Rat hepatitis E virus derived from wild rats (Rattus rattus) propagates efficiently in human hepatoma cell lines. *Virus Res* **185**, 92-102, 2014.
43. Tanggis, Kobayashi, T., Takahashi, M., Jirintai, S., Nishizawa, T., Nagashima, S., Nishiyama, T., Kunita, S., Hayama, E., Tanaka, T., Mulyanto & Okamoto, H. An analysis of two open reading frames (ORF3 and ORF4) of rat hepatitis E virus genome using its infectious cDNA clones with mutations in ORF3 or ORF4. *Virus Res* **249**, 16-30, 2018.
44. Tanaka, T., Takahashi, M., Kusano, E. & Okamoto, H. Development and evaluation of an efficient cell-culture system for hepatitis E virus. *J Gen Virol* **88**, 903-911, 2007.
45. Lorenzo, F. R., Tanaka, T., Takahashi, H., Ichiyama, K., Hoshino, Y., Yamada, K., Inoue, J., Takahashi, M. & Okamoto, H. Mutational events during the primary propagation and consecutive passages of hepatitis E virus strain JE03-1760F in cell culture. *Virus Res* **137**, 86-96, 2008.
46. Kobayashi, T., Takahashi, M., Tanggis, Mulyanto, Jirintai, S., Nagashima, S., Nishizawa, T. & Okamoto, H. Characterization and epitope mapping of monoclonal antibodies raised against rat hepatitis E virus capsid protein: an evaluation of their neutralizing activity in a cell culture system. *J Virol Methods* **233**, 78-88, 2016.
47. Takahashi, M., Kobayashi, T., Tanggis, Jirintai, S., Mulyanto, Nagashima, S., Nishizawa, T., Kunita, S. & Okamoto, H. Production of monoclonal antibodies against the ORF3 protein of rat hepatitis E virus (HEV) and

demonstration of the incorporation of the ORF3 protein into enveloped rat HEV particles. *Arch Virol* **161**, 3391-3404, 2016.

48. Urata, S., Noda, T., Kawaoka, Y., Yokosawa, H. & Yasuda, J. Cellular factors required for Lassa virus budding. *J Virol* **80**, 4191-4195, 2006.
49. Yasuda, J., Nakao, M., Kawaoka, Y. & Shida, H. Nedd4 regulates egress of Ebola virus-like particles from host cells. *J Virol* **77**, 9987-9992, 2003.
50. Mulyanto, Suparyatmo, J. B., Andayani, I. G., Khalid, Takahashi, M., Ohnishi, H., Jirintai, S., Nagashima, S., Nishizawa, T. & Okamoto, H. Marked genomic heterogeneity of rat hepatitis E virus strains in Indonesia demonstrated on a full-length genome analysis. *Virus Res* **179**, 102-112, 2014.
51. Takahashi, M., Hoshino, Y., Tanaka, T., Takahashi, H., Nishizawa, T. & Okamoto, H. Production of monoclonal antibodies against hepatitis E virus capsid protein and evaluation of their neutralizing activity in a cell culture system. *Arch Virol* **153**, 657-666, 2008.
52. Sasaki, J., Kusuhara, Y., Maeno, Y., Kobayashi, N., Yamashita, T., Sakae, K., Takeda, N. & Taniguchi, K. Construction of an infectious cDNA clone of Aichi virus (a new member of the family Picornaviridae) and mutational analysis of a stem-loop structure at the 5' end of the genome. *J Virol* **75**, 8021-8030, 2001.
53. Ostrowski, M., Carmo, N. B., Krumeich, S., Fanget, I., Raposo, G., Savina, A., Moita, C. F., Schauer, K., Hume, A. N., Freitas, R. P., Goud, B., Benaroch, P., Hacohen, N., Fukuda, M., Desnos, C., Seabra, M. C., Darchen, F., Amigorena, S., Moita, L. F. & Thery, C. Rab27a and Rab27b control different steps of the exosome secretion pathway. *Nat Cell Biol* **12**, 19-30; sup pp 11-13, 2010.
54. Tamai, K., Tanaka, N., Nakano, T., Kakazu, E., Kondo, Y., Inoue, J., Shiina, M., Fukushima, K., Hoshino, T., Sano, K., Ueno, Y., Shimosegawa, T. & Sugamura, K. Exosome secretion of dendritic cells is regulated by Hrs, an ESCRT-0 protein. *Biochem Biophys Res Commun* **399**, 384-390, 2010.
55. Alvarez-Erviti, L., Seow, Y., Schapira, A. H., Gardiner, C., Sargent, I. L., Wood, M. J. & Cooper, J. M. Lysosomal dysfunction increases exosome-mediated alpha-synuclein release and transmission. *Neurobiol Dis* **42**, 360-367, 2011.

56. Trajkovic, K., Hsu, C., Chiantia, S., Rajendran, L., Wenzel, D., Wieland, F., Schwille, P., Brugger, B. & Simons, M. Ceramide triggers budding of exosome vesicles into multivesicular endosomes. *Science* **319**, 1244-1247, 2008.

57. Gottlinger, H. G., Dorfman, T., Sodroski, J. G. & Haseltine, W. A. Effect of mutations affecting the p6 gag protein on human immunodeficiency virus particle release. *Proc Natl Acad Sci U S A* **88**, 3195-3199, 1991.

58. Kenney, S. P., Pudupakam, R. S., Huang, Y. W., Pierson, F. W., LeRoith, T. & Meng, X. J. The PSAP motif within the ORF3 protein of an avian strain of the hepatitis E virus is not critical for viral infectivity in vivo but plays a role in virus release. *J Virol* **86**, 5637-5646, 2012.

59. Hanson, P. I. & Cashikar, A. Multivesicular body morphogenesis. *Annu Rev Cell Dev Biol* **28**, 337-362, 2012.

60. Morita, E., Sandrin, V., McCullough, J., Katsuyama, A., Baci Hamilton, I. & Sundquist, W. I. ESCRT-III protein requirements for HIV-1 budding. *Cell Host Microbe* **9**, 235-242, 2011.

61. Pawliczek, T. & Crump, C. M. Herpes simplex virus type 1 production requires a functional ESCRT-III complex but is independent of Tsg101 and Alix expression. *J Virol* **83**, 11254-11264, 2009.

62. Tamai, K., Shiina, M., Tanaka, N., Nakano, T., Yamamoto, A., Kondo, Y., Kakazu, E., Inoue, J., Fukushima, K., Sano, K., Ueno, Y., Shimosegawa, T. & Sugamura, K. Regulation of hepatitis C virus secretion by the Hrs-dependent exosomal pathway. *Virology* **422**, 377-385, 2012.

63. Mori, Y., Koike, M., Moriishi, E., Kawabata, A., Tang, H., Oyaizu, H., Uchiyama, Y. & Yamanishi, K. Human herpesvirus-6 induces MVB formation, and virus egress occurs by an exosomal release pathway. *Traffic* **9**, 1728-1742, 2008.